Sustainable Materials and Technologies 45 (2025) e01477

Contents lists available at ScienceDirect

Sustainable Materials and Technologies

journal homepage: www.elsevier.com/locate/susmat

Catalytic effect of mixed oxides in phosphine oxide epoxy-based covalent adaptable networks: Recyclability, fire protection, and smoke suppression☆

Valeria Palumbo [a,b], Wenyu Wu Klingler [a,*], Nikita Drigo [a], Ton Markaj [a], Aurelio Bifulco [b,*], Claudio Imparato [b], Alex Imboden [a], Sandro Lehner [a], Alessia Arpaia [a,b], Elisabetta Finocchio [c], Antonio Aronne [b], Sabyasachi Gaan [a,*]

[a] Laboratory for Advanced Fibers, Empa Swiss Federal Laboratories for Materials Science and Technology, Lerchenfeldstrasse 5, 9014 St. Gallen, Switzerland
[b] Department of Chemical, Materials and Production Engineering (DICMaPI), University of Naples Federico II, P.le Tecchio 80, 80125 Naples, Italy
[c] Department of Civil, Chemical and Environmental Engineering, University of Genoa, Via Opera Pia 15, 16145 Genoa, Italy

ARTICLE INFO

Keywords:
Covalent adaptable network
Epoxy vitrimer
Dynamic bond exchange
Solid acid catalyst
Reprocessability
Flame retardancy

ABSTRACT

The non-recyclable nature and high flammability are two significant shortcomings of epoxy thermosets. Designing inherently flame-retardant epoxy-based composites with covalent adaptable networks (CANs) can counteract these issues. A new diphenyl phosphine oxide containing dicarboxylic acid (DPPOIPA) is synthesized and used with citric acid as hardeners to prepare inherently flame retardant epoxy polyester vitrimers. Sol-gel derived binary (Nb_2O-SiO_2, SiNb; P_2O_5-SiO_2, SiP) and ternary (Nb_2O_5-P_2O_5-SiO_2, SiNbP) acid solids are employed as transesterification catalysts and co-flame retardants to promote dynamic bond exchange and flame retardancy of the thermoset matrix. These mixed oxides lower the activation energy for the crosslinking reactions, resulting in efficient esterification during initial curing. The epoxy polyester vitrimers, containing a very low P amount (~2 wt%), exhibit thermomechanical recyclability, flame self-extinguishing (V-0 rating at the UL 94 vertical burning test), and no dripping capability. However, vitrimers containing conventional zinc acetate only achieve a V-1 class, even with the same P content. Among the prepared catalysts, SiNbP allows for a substantial reduction in the peak heat release rate (pHRR), which is approximately 63 % lower than that of the pristine thermoset, accompanied by a remarkable increase (~70 %) in the time to ignition, clearly indicating its intense condensed-phase flame retardant action. It is worth mentioning that a notable decrease in the total smoke release (up to 62 %) occurs in all samples containing mixed oxides, either in the presence or absence of DPPOIPA. Due to the suitable distribution of acid sites, SiNbP also enhances the release of phosphorus radicals, which is attributed to the decomposition of DPPOIPA, resulting in a strong inhibition effect in the gas phase. Strikingly, despite this effect in the gas phase, the release of smoke in the fire does not increase, thanks to the catalytic effect of the mixed oxides. This work reveals that acidic mixed oxides can be effective and sustainable bifunctional additives in epoxy polyester vitrimers, acting as solid catalysts for their recycling, smoke suppression, and fire protection.

1. Introduction

Polymers are widely employed in daily life and several industrial applications due to their low cost and versatility [1,2]. Thermosets are polymers composed of permanent networks, which are usually obtained by the reaction of a monomer with a curing agent, giving them high chemical stability, adhesive, and mechanical properties. Stringent fire safety regulations require the use of flame retardant functional thermoset composites in transportation, construction, and electrical components [3,4]. Unlike thermoplastics, thermosets cannot be reprocessed and thermally reshaped, as they undergo degradation at high temperatures, and thus their recycling is full of hurdles and very challenging [5,6]. Besides, the presence of residual flame retardants (FRs) in thermosetting wastes needs to be considered, as these FRs may cause the release of toxic species into the environment during their recycling [7]. In fire-safe applications of thermosets, for example, in

☆ This article is part of a Special issue entitled: 'Sustainable fire-retardant materials' published in Sustainable Materials and Technologies.

* Corresponding authors.
E-mail addresses: wenyu.wu@empa.ch (W. Wu Klingler), aurelio.bifulco@unina.it (A. Bifulco), sabyasachi.gaan@empa.ch (S. Gaan).

https://doi.org/10.1016/j.susmat.2025.e01477
Received 21 March 2025; Received in revised form 20 May 2025; Accepted 4 June 2025
Available online 5 June 2025

epoxy resins, phosphorus(P)-based FRs have mainly been explored to lower their flammability [8–10]. Satisfactory fire performances and non-leaching behavior were obtained by the application of reactive P-based FRs, such as 9,10-dihydro-9-oxa-10-phosphaphenanthrene-10-oxide (DOPO) [11–13]. At the end of their life, these FR thermosets are mostly burned or landfilled, causing the depletion of precious raw materials and phosphorus, which is estimated to run out in a few decades [5,14]. Given that, extending the life cycle of FR epoxy materials and conferring them recyclable and sustainable features is an urgent challenge to address from the circular economy's perspective. To resolve this challenge, Leibler's group invented "vitrimers," materials made up of covalent adaptable networks (CANs) [15–17], which could be reprocessed or repaired thanks to the presence of reversible dynamic crosslinks within the polymer matrix, enabling the topological rearrangement of the thermoset network under specific external stimuli (e.g., pH, heat radiation) [18,19]. In the literature, several types of recyclable thermosets made of CANs can be found, including disulfide [20], dioxaborolane [21], carboxylic ester [22], imine [23], etc. These CANs endow the material with reprocessing properties, enabling its thermomechanical or chemical recycling under specific working conditions by facilitating bond exchange.

Phosphate ester-based vitrimers are drawing great interest due to the flexibility of phosphates' chemistry, which can lead to the production of many reactive monomers [24]. However, as confirmed by aging experiments, phosphates are unstable to hydrolysis, which strongly limits the possible use of phosphate ester-based vitrimers in the industry [11,25,26]. To overcome such drawback, phosphate esters may be replaced with phosphonates or phosphine oxides to obtain non-hydrolysable P—C bonds and more thermally stable materials [27–29]. Klingler et al. synthesized a thermomechanically easy-to-recycle phosphonate-based epoxy thermoset, showing good fire behavior and no leaching during end-of-life treatment [30]. On the other hand, a partially bio-based phosphine oxide monomer (diphenylphosphine oxide itaconic anhydride) was shown to endow bisphenol A diglycidyl ether (DGEBA) based carboxylic ester networks with excellent reprocessability and repairability, enhanced flexural strength, and self-extinguishment [31].

In a hydroxy-ester vitrimer network, the dynamic bond exchange occurs through a transesterification reaction involving an alkoxy exchange between two reaction centers, the reactant ester, and alcohol [32]. The transesterification reaction occurs preferably in the presence of either an acid or basic catalyst. When an acid catalyst is used, it draws electrons away from the carbonyl moiety of the ester, making it a stronger electrophile, prone to nucleophilic attack. On the other side, a basic catalyst acts as an electron-donating group enhancing the nucleophilicity of the alkoxy oxygen of the alcohol [32]. To date, zinc complexes, such as Zn(II) acetate, are the most primarily employed catalysts in the manufacturing of epoxy vitrimers based on transesterification reaction [25,32–35], although loads up to 10 wt% or larger are sometimes needed [35,36]. Some researchers have tried to elucidate further the role of catalyst's features in the bond exchange of polyester CANs [37,38]. Recent experimental and theoretical studies found that transesterification benefits from the coexistence of acid and basic sites on suitable catalysts [32], and that strong Brønsted acids favour it [39]. Although some alternative catalysts have been investigated, the literature still lacks information on additives that can simultaneously enable recyclability, promote bond exchange, and improve the flame retardancy of epoxy thermosets.

In industrial processes, inorganic heterogeneous catalysts are generally preferred to homogeneous systems and materials containing organic moieties, as they maintain their integrity at high pressures and temperatures, reducing the costs linked to recovery and reusability [40]. Transition metal oxides and phosphates are well-known solid acidic catalysts. Intending to combine the acidic characteristics of niobium and phosphorus with porous silica support, we synthesized Si-Nb-P ternary oxides by a hydrolytic sol-gel route [41]. These materials showed a tunable distribution of Brønsted and Lewis acid sites, variable acid strength, and enhanced resistance of phosphate species toward leaching in water, owing to the formation of Si–O–Nb–O–P linkages. These properties led to excellent catalytic performances in acid-catalyzed reactions such as esterification, hydrolysis, and dehydration [41–43]. Such Si-Nb-P ternary oxides may represent an appealing alternative to traditional catalysts in the preparation of vitrimers. Also, the strong acidity of these materials may boost the dehydration of the polymer matrix, promoting the formation of a thermally stable char in the condensed phase able to act as thermal shield and oxygen barrier during the combustion. Therefore, mixed oxides may exert a double role, thanks to their peculiar chemical characteristics, acting as flame retardants during combustion and as catalysts during thermomechanical recycling. In addition, their inorganic nature would allow reprocessing even at harsh temperature conditions, as in the case of high performing polymers. On the other hand, the development of inherently FR and recyclable thermosets, in which the chemical moieties that make the polymer recyclable are the same giving it FR properties, is recently raising great attention [25,44,45].

Herein, inherently recyclable and flame retardant epoxy vitrimers were obtained by curing DGEBA with a new diphenyl phosphine oxide compound bearing two carboxylic groups (DPPOIPA, Scheme 1) and incorporating three acid solids as heterogeneous catalysts for the transesterification reaction. The solid acid materials (Si—Nb—P, Si—P, and Si—Nb oxides) were synthesized by sol-gel methodology, and the nature and distribution of their acid sites were determined by in situ FTIR spectroscopy of adsorbed probe molecules. The combined presence of DPPOIPA and acid solids guarantees good thermomechanical recyclability of the epoxy vitrimers. The UL 94 vertical burning test attested the no-dripping V-0 rating for the prepared materials, even with a low P content (2 wt%), without or with the solid catalysts. These results confirm the potentiality of acid solids in playing a double function as transesterification catalysts and flame retardants in epoxy-based vitrimers.

2. Experimental

2.1. Materials

Epoxy resin (EP, DGEBA, Epikote™ Resin 827) was provided by Hexion Specialty Chemicals GmbH, Germany. Citric acid (99.5 %, AR) was purchased from Combi-Blocks, Chemie Brunschwig AG, Switzerland. Diphenylphosphine oxide (DPPO) and starting materials employed for the synthesis of 5-(diphenylphosphoryl)isophthalic acid were acquired from Sigma-Aldrich (Switzerland) and used as received. All synthesis operations involving air sensitive reagents and materials were performed employing the Schlenk techniques. Binary (SiNb, SiP) and ternary (SiNbP) oxides, tested as solid acid catalysts in the vitrimeric systems, were synthesized by a sol-gel method using as precursors tetraethyl orthosilicate (TEOS, 98 %), ammonium niobium oxalate hydrate, $NH_4[NbO(C_2O_4)_2(H_2O)_2]\bullet nH_2O$ (ANO), and orthophosphoric acid (85 wt% solution), all supplied by Sigma-Aldrich.

2.2. Synthesis of 5-(diphenylphosphoryl)isophthalic acid (DPPOIPA)

The reaction steps for the synthesis of DPPOIPA are illustrated in Scheme 1. In a typical preparation procedure, a three-neck round bottom flask with a mechanical stirrer, including a N_2 inlet, a thermometer and a condenser, is charged with triphenylphosphine (178.88 g, 0.682 mol), 1-bromo-3,5-dimethylbenzene (114.74 g, 0.620 mol, Br-DMIPA), nickel chloride (2.41 g, 0.0186 mol) and ethylene glycol (600 mL) at room temperature. The reaction mixture is then heated up to 180 °C while stirring. The color of the emulsion changes from yellow to green darkens over time and finally becomes orange-brown. At first, the reaction mixture consists of two phases, and then the system becomes homogenous. The reaction mixture is stirred for 16 h under nitrogen and

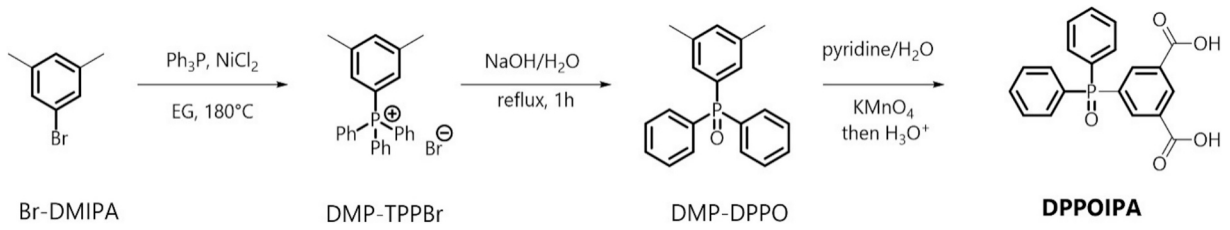

Scheme 1. Reaction pathway for synthesizing 5-(diphenylphosphoryl)isophthalic acid (DPPOIPA) from 1-bromo-3,5-dimethylbenzene.

allowed to cool down as soon as a brown color indicates the completion of the reaction. Then, dichloromethane (200 mL) and deionized H_2O (100 mL) are added to the mixture to separate the organic phase. The organic phase is washed three times with 200 mL of diluted HBr (0.35 vol%), dried over Na_2SO_4, filtered, and then concentrated to approximately 1/3 of its initial volume. The concentrate is then placed into a dropping funnel and added to 200 mL of 2-methoxy-2-methylpropane (MTBE) up on vigorous stirring. The precipitate formed is then collected and washed twice with 200 mL of MTBE. The resulting product is collected and dried at 80 °C overnight under vacuum to obtain a white-yellowish powder with 85–90 % yield of (3,5-dimethylphenyl) triphenylphosphor bromide (DMP-TPP-Br in Scheme 1).

In the subsequent step, a three-neck round bottom flask equipped with a mechanical stirrer, an N_2 inlet, a thermometer, and a condenser is charged with deionized H_2O (600 mL) at room temperature. Then sodium hydroxide (108.34 g, 2.71 mol) is added portion-wise, since its dissolution is very exothermic. DMP-TPPBr is added portion-wise into the alkali solution upon stirring. The reaction mixture is refluxed for 1 hand then allowed to cool down. Afterwards, dichloromethane (800 mL) is added to the mixture. The organic phase is washed three times with 200 mL of deionized H_2O, dried over Na_2SO_4, filtered, and the solvent is removed under reduced pressure. The resulting product is collected and dried at 80 °C overnight under vacuum to obtain a white-yellowish solid with 95–98 % yield of (3,5-dimethylphenyl)diphenylphosphine oxide (DMP-DPPO in Scheme 1).

In the final step, a three-neck round bottom flask, equipped with a mechanical stirrer, a thermometer and a condenser, is charged with DMP-DPPO (136.6 g, 0.446 mol) and pyridine (400 mL) at room temperature. The reaction mixture is then stirred until the solid is fully dissolved. After that, deionized H_2O (800 mL) is carefully added in small portions. The mixture is heated up to 90 °C while stirring. The oxidation reaction is exothermic and sometimes causes effervescence. Therefore, care must be taken to gradually add finely ground $KMnO_4$ (704.7 g, 4.46 mol). After deionized water (600 mL) is added to the mixture, it is refluxed overnight. After completion, the mixture is allowed to cool down and the excess of $KMnO_4$ is quenched with MeOH (500 mL). The remaining MnO_2 is then filtered off and washed thoroughly with water. The resulting solution is evaporated to approximately 1/3 of the initial volume, so a white solid precipitates. The concentrate is then acidified to pH ≈ 1 with HCl until no more precipitate forms upon adding new portions of HCl. Care must be taken upon adding the inorganic acid because the reaction is exothermic and releases gas while reaching low pH. The resulting product is collected and dried at 80 °C overnight under vacuum to obtain a white-yellowish solid with 90–92 % yield of 5-(diphenylphosphoryl)isophthalic acid (DPPOIPA in Scheme 1).

The synthesized products were analyzed using NMR, and the spectra of DPPOIPA are shown in the supplementary information (see Fig. S1). ^{1}H NMR (400 MHz, Acetone-d_6) δ 8.72 (brs, 2H), 7.37 (dd, J = 8.5, 2.0 Hz, 4H), 7.14 (d, J = 2.4 Hz, 4H), 6.80 (d, J = 8.5 Hz, 4H). ^{13}C NMR (101 MHz, Acetone-d_6) δ 141.01, 137.40, 136.42, 132.84, 117.44, 82.30. HRMS (MALDI-TOF-MS): calcd. for $[M]^+$ $C_{25}H_{14}I_4N_2$: 849.7336; found 849.732.

2.3. Synthesis of the mixed oxides

The adopted procedures are based on the green hydrolytic sol-gel route established for the Si-Nb-P ternary oxides [41]. To obtain the SiNbP sample, ANO is dissolved in deionized water, and then the solution is mixed with TEOS under stirring. After 1 h, H_3PO_4 is added, and the resulting clear solution is stirred at room temperature until gelation. The acidity of ANO and H_3PO_4 promotes TEOS hydrolysis without the need for additional acid catalysts. The SiNb binary sample is synthesized by an analogous procedure, without introducing H_3PO_4 to the ANO-TEOS aqueous solution. In the case of the SiP binary oxide, ethanol is used as a solvent with a lower amount of water in order to moderate the hydrolysis and condensation rate and preserve the Si-O-P crosslinking. Indeed, the sensitivity of Si-O-P linkages to hydrolysis makes the sol-gel processing of phosphosilicate gels in water environment challenging [26]. Quantitative details are reported in Table S1. Clear homogeneous gels are obtained for all three systems in about 3 days. The gels are kept aging at room temperature for 2 days, then thoroughly dried in air at 110 °C. Finally, the xerogels are ground by ball milling and calcined in air at 500 °C for 1 h at the heating rate of 10 °C min^{-1}. The nominal molar compositions of the three mixed oxides are the following: $92.5SiO_2{\cdot}2.5Nb_2O_5{\cdot}5P_2O_5$ (SiNbP); $97.5SiO_2{\cdot}2.5Nb_2O_5$ (SiNb); $95SiO_2{\cdot}5P_2O_5$ (SiP). The corresponding mass compositions are reported in Table S2.

Table 1
Composition of the studied epoxy-based samples.

Sample	DGEBA (mol)	CA/DGEBA (mol/mol)	DPPOIPA/DGEBA (mol/mol)	Catalyst (10 wt% of precured resin)	Final P content (wt.%)*
EV	1	0.67	–	–	–
EV-SN	1	0.67	–	SiNb	–
EV-SP	1	0.67	–	SiP	–
EV-SNP	1	0.67	–	SiNbP	–
EVP	1	0.40	0.40	–	2.0
EVP-Zn	1	0.40	0.40	$Zn(OAc)_2$	2.2
EVP-SN	1	0.40	0.40	SiNb	1.8
EVP-SP	1	0.40	0.40	SiP	2.2
EVP-SNP	1	0.40	0.40	SiNbP	2.4

* Final P content was measured by ICP-OES.

2.4. Preparation of epoxy-based vitrimers

The composition of each formulation is reported in Table 1. In a typical preparation, epoxy resin was mixed with DPPOIPA, citric acid, and the catalyst in a beaker and cured using a one-pot and solvent-free approach [31]. It is essential to highlight here that all solid ingredients need to grinded fine powder either with a mechanical grinder or a cryomill. Citric acid was selected as a bio-based co-curing agent to establish a carboxylic ester-based network that can be rearranged by the activation of dynamic exchangeable bonds topologically. Both citric acid and DPPOIPA can act as curing agents through the carboxylic groups. All the solid starting materials first underwent a cryo-milling process to achieve micron-sized particles and promote uniform mixing. A mixture of DGEBA and hardeners was heated at 60 °C in a water bath. Subsequently, the catalyst, either SiNb, SiP or SiNbP, was added, and the mixture was stirred at 60 °C until it appeared homogeneous. The molar composition of the studied systems is DGEBA:CA:DPPOIPA = 1.0:0.4:0.4, ensuring an equal molar ratio between the carboxylic and oxirane groups. The catalyst content of 10 wt% of precured DGEBA was proven to be the optimal value by preliminary tests. The nominal P content in the polymer matrix of these composites is about 2.0 wt% (Table 1). The cure was performed by heating the samples in the moulds at 110 °C for one hour, 140 °C for 2 h, and then at 160 °C for 2 h. The curing conditions were determined based on carefully evaluating the activation temperature and energy of the esterification reactions, carried out by differential scanning calorimetry (DSC). The possible structure of the obtained polyester vitrimer is represented in Scheme 2. The samples are labelled "EVP" followed by the short name of the catalyst. Two reference samples were prepared: EVP without any catalyst and EVP-Zn containing the conventional zinc acetate ($Zn(OAc)_2$) catalyst (Table 1). Also, a set of samples was synthesized with DGEBA: CA molar ratio 1:0.67, to keep the molar ratio between the carboxylic and oxirane groups equal to 1, and no DPPOIPA, labelled "EV". Afterward, the cured samples were used to investigate the thermal, fire, and recycling performances.

2.5. Characterization of the mixed oxides

The structural and surface properties of the synthesized silica-based oxides (SiNb, SiP, and SiNbP) were investigated by X-ray diffraction (XRD), thermogravimetric and differential thermal analysis (TG-DTA), Fourier transform infrared (FTIR) spectroscopy. Their acidity was assessed by the IR analysis of surface species following pyridine adsorption, carried out using pure powder self-supporting disks in the IR cell connected to a gas-manipulation apparatus, previously described [46]. Experimental details are reported in the Supporting Information (Section S1).

2.6. Characterization of the epoxy-based vitrimers

The phosphorus content in the studied epoxy samples was measured with inductively coupled plasma optical emission spectroscopy (ICP-OES). The thermal properties of the composites were assessed with TGA and DSC. The curing kinetics of the formulations were studied with DSC runs at four different heating rates (5, 10, 15, and 20 °C min^{-1}), and the activation energies were determined following the Kissinger Eq. [47]:

$$\ln\frac{\beta}{T^2} = \ln\frac{AR}{E_a} - \frac{E_a}{RT} \quad (1)$$

where β is the heating rate, T is the peak (or onset) temperature, corresponding to the maximum rate (or initial) of the curing process, A is the pre-exponential factor, E_a is the activation energy and R is the universal gas constant.

All the prepared samples were analyzed by FTIR spectroscopy in ATR mode, SEM-EDX analysis, UL 94 vertical burning tests, cone calorimetry (CC), and pyrolysis combustion flow calorimetry (PCFC). Gas evolved analysis was performed by direct inlet probe mass spectrometry (DIP-MS). Details about each characterization methodology are reported in the Supporting Information (Section S1).

2.7. Thermomechanical reprocessing

The recyclability of the vitrimers was tested through a thermo-mechanical reprocessing. First, mechanical centrifugal griding and cryomilling processes were performed to reduce the materials into granules, and then into fine powder. The use of the cryogenic mill is crucial, as a smaller particle size leads to a final sample with lower porosity [48]. Then, a hot press was used: the obtained powder was placed in a metal mould and pressed between two heating plates. The various samples have been reprocessed at 250 °C for maximal one hour to give satisfactory results. The pressure sequence was the same for each sample, going through the following steps: 0.5 tons, 4 tons, 10 tons, and 25 tons. During this thermal compression, particles fuse thanks to thermally stimulated network rearrangement. The reprocessed samples, labelled with the name of the sample followed by underscore R, "_R", were characterized by FTIR-ATR, TGA, DSC, as described above.

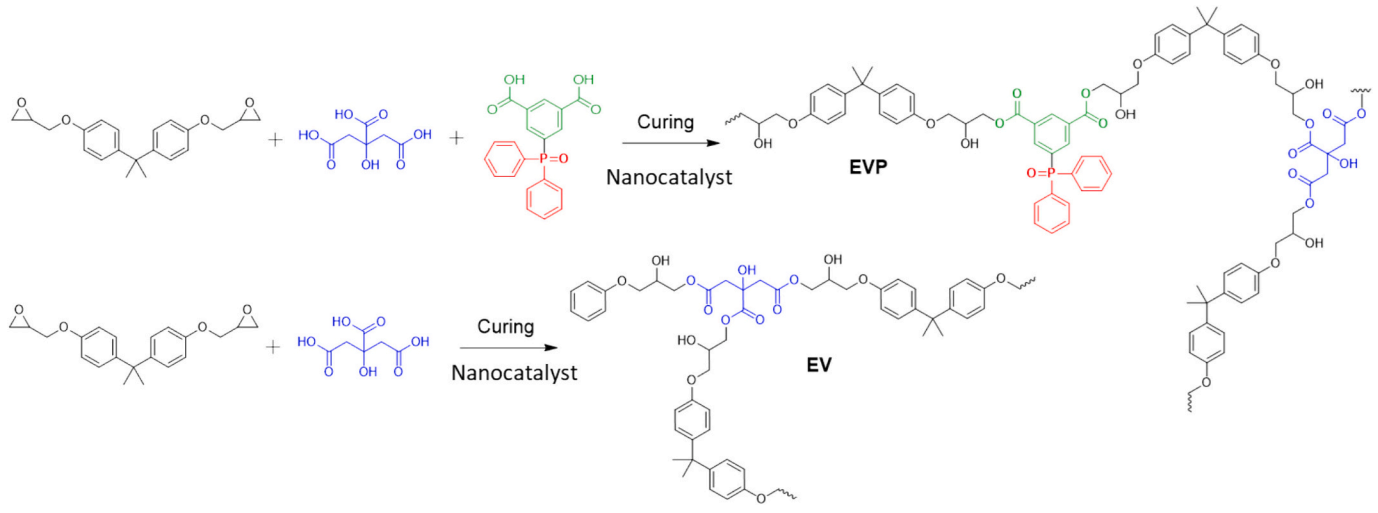

Scheme 2. Synthetic route of EVP series with DPPOIPA as co-curing reagent, and the blank EV, with the molecular structure of DGEBA, DPPOIPA (with the pendant group in red), citric acid and simplified illustration of the epoxy-based network formed by ester bonds in presence of the nanocatalysts (SiP, SiNb or SiNbP).

3. Results and discussion

3.1. Structural and acid properties of the mixed oxides

The synthesized binary (SiNb and SiP) and ternary (SiNbP) oxides are constituted by a silicon oxide network in which niobium and phosphorus units are dispersed. The powders have an essentially amorphous structure, as attested by XRD patterns (Fig. S2), which suggest the absence of segregated Nb_2O_5 or P_2O_5 crystalline phases. Only SiNbP shows very weak diffraction peaks emerging from the halo of the amorphous matrix at 2θ about 19 and 28°. These can be attributed to small crystallites of niobium oxophosphate ($NbOPO_4$) [49], though they are also compatible with phases richer in P, such as $Nb_5P_7O_{30}$ [50]. $NbOPO_4$ is a well-known acidic solid characterized by a strong intrinsic Lewis/Brønsted acidity and good thermal stability [51].

FTIR skeletal spectra (Fig. 1a) show the main band due to the silica network at 1050 cm^{-1} with a shoulder at 1180 cm^{-1}, assigned to the asymmetric stretching mode of Si–O–Si groups. The peaks at 797 and 450 cm^{-1} (ill-defined) are assigned to the corresponding symmetric stretching and deformation modes. The shoulder at 960 cm^{-1} ca. can be related to the deformation mode of Si–OH, indicating that isolated silanols are present at the catalyst surface [42]. No bands due to organic compounds are detected in the spectra of the calcined samples, in agreement with TGA results. The TGA curves (Fig. S3) confirm that the calcination at 500 °C removes the organic components of the gels, stabilizing the ceramic structure. All the materials undergo a single main mass loss below 130 °C, due to the vaporization of adsorbed water. The extent of this loss (about 12, 15 and 16 wt% for SiNb, SiP and SiNbP, respectively) testifies a significant hydrophilicity of the solid surfaces, especially those containing phosphate. The subsequent gradual mass decrease of about 4 wt% is attributed to dehydroxylation phenomena, that is, the condensation of surface hydroxyl groups with formation of new oxo bridges and elimination of water molecules. A representation of the envisaged structure of the mixed oxides is shown in Fig. 1c.

The surface acid properties of the silica-based oxides were investigated by the adsorption of pyridine (PY). PY is a basic compound both in water solution and in gas-phase interaction, having the pK_a of the conjugated acid equal to 5.2 and a proton affinity equal to 912 kJ/mol [52], and it is usually applied as a probe to evaluate the nature of exposed acidic sites over solid catalysts. Indeed, ternary and binary oxides surfaces are complex, and PY can interact with them in several ways. A Brønsted acidic site (B) able to protonate pyridine gives rise to

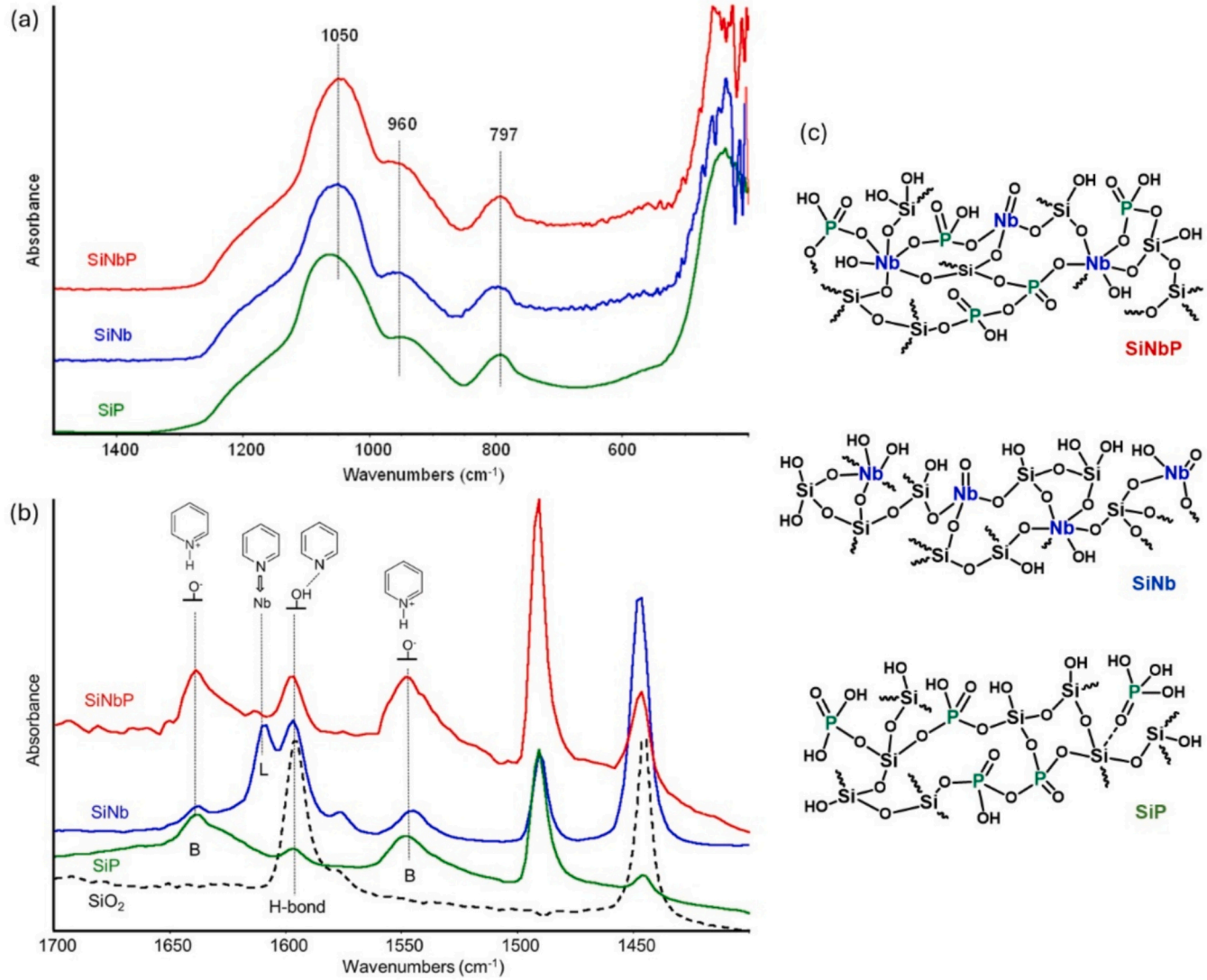

Fig. 1. (a) ATR-IR skeletal spectra of the synthesized mixed oxide powders. (b) FTIR subtraction spectra of surface species arising from pyridine adsorption and outgassing at 150 °C on mixed oxides and reference SiO_2, prepared by sol-gel from TEOS in similar conditions to the other samples. The activated surface spectrum has been subtracted. (c) Representative illustration of the surface layers of SiNbP, SiNb and SiP.

pyridinium ions, PYH^+, whose diagnostic IR bands fall at 1635 and 1545 cm^{-1}. PY can also coordinate at Lewis sites (L), which behave as electron-withdrawing centers, and in this case sensitive bands are located at 1610–20 cm^{-1} and near 1450 cm^{-1}. Other IR components are centred near 1590 and 1445 cm^{-1}, assigned to pyridine hydrogen-bonded and weakly interacting with silanol groups (HPY). These bands usually disappear after outgassing at increasing temperature. Over the samples analyzed in this study, spectra arising from PY adsorption and desorption at 150 °C are reported in Fig. 1b, where the main IR bands diagnostic of different interactions have been highlighted.

These results show that the surface of SiP is mainly characterized by Brønsted acidity and weakly acidic silanol groups. As suggested previously [53], the strongest acidic contribution to the catalytic activity of silicophosphate materials can be due to P–OH species and some Si–OH species, whose acidity is enhanced by nearby PO groups. On the other side, the surface of SiNb shows both exposed Brønsted and medium strength Lewis acidic sites, associated to the presence of Nb-OH and coordinatively unsaturated Nb(V) sites, respectively [51]. Finally, PY adsorption over SiNbP ternary system leads to similar conclusions: the surface mainly shows Brønsted acidity (diagnostic bands at 1639 and 1548 cm^{-1}) and weak acidity due to silanols. Moreover, the presence of Nb adds some Lewis acidity (weak shoulder at 1612 cm^{-1}). Over this material, the relative concentration of Brønsted acid sites, evaluated by comparing the intensities of bands at 1545 cm^{-1} (B) and 1445 cm^{-1} (L), is by far higher than in the SiNb binary sample, although some amount of exposed Nb species is also present, behaving as Lewis sites (see Fig. 1c). Thus, the surface of the ternary oxide shows a combination of protonic and coordinatively unsaturated acidic sites.

3.2. Formation of the dynamic crosslinked network

The reaction of DGEBA with carboxylic acids produces 2-hydroxyester chains through nucleophilic attack on the epoxide ring, as represented in Scheme 2. However, this is a simplified picture, as other reactions may occur in parallel or in series, forming crosslinks, especially involving free hydroxyl groups, for example their esterification with carboxylic groups, their transesterification with ester bonds, and their reaction with epoxide rings [34,54]. The thermal curing of the prepared epoxy resins was investigated by means of DSC. The study of the curing kinetics is important for ensuring the processability and optimizing the curing cycle conditions, which determine the final properties of the product. In our case, it was also aimed to evaluate the effect of the different catalysts on the crosslinking of the polymer matrix. A model-free kinetic method was chosen, since it hypothesizes that the reaction rate at constant conversion degree is simply a function of the temperature, without assuming a specific reaction mechanism [55]. Representative DSC curves measured at different heating rates are shown in Fig. 2a–e. As expected, the broad exothermic peak related to crosslinking reactions shifts to higher temperatures and grows in magnitude as the heating rate increases [56]. Based on these data, a curing protocol was established, namely a step at 140 °C for 2 h, followed by post-cure at 160 °C for 2 h. In the DSC profiles of all samples a small endothermic peak is seen at about 155 °C, likely due to the melting of some unreacted citric acid. The activation energies (E_a) for the curing process of each sample, estimated by Kissinger method (Eq. 1) are reported in Table S3 and shown in Fig. 2f. It is worth noting that the incorporation of DPPOIPA in the epoxy system causes a significant drop (27 %) in the E_a value with respect to EV reference sample, that may be related to better chemical affinity of DPPOIPA than CA toward DGEBA giving an overall decrease of the energy barrier. This suggests that EVP materials could also show a better reprocessability through transesterification reactions.

As highlighted in Fig. 2f, all the heterogeneous catalysts provide lower E_a than bare EV and EVP, with the extent of the decrease following the order: EVP-SP < EVP-SN < EVP-SNP. The synthesized mixed oxides appear effective in catalyzing the esterification reactions, affording lower E_a (up to 36 %) than the one of EVP, probably due to their

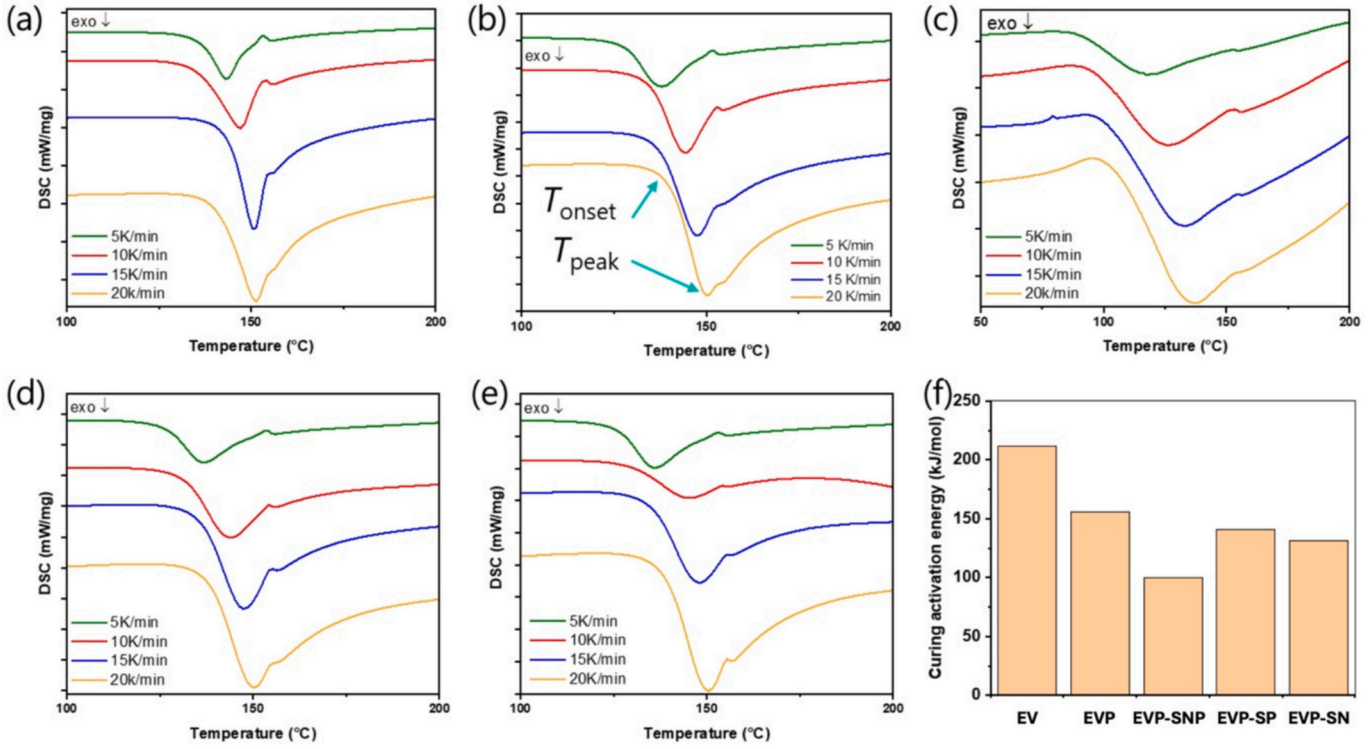

Fig. 2. DSC curing curves of the epoxy-based polyester systems recorded in nitrogen at different heating rates, including (a) the control sample EV, (b) EVP, (c) EVP-SNP, (d) EVP-SP, (e) EVP-SN, and (f) the curing activation energies for obtaining crosslinked polymeric matrix without and with different catalysts, estimated by the Kissinger equation as an average between the values obtained from peak temperatures.

significant acidity and a suitable combination of acid sites. This result hints at the possible efficiency of these catalysts in promoting, under favorable operating conditions, a topological rearrangement based on transesterification reactions, enabling the thermoset's chemical recycling.

3.3. Structural and thermal analysis of the epoxy-based vitrimers

The chemical structure of the prepared epoxy resins was analyzed by ATR-FTIR spectroscopy. The spectra of the precursors, i.e. DGEBA, CA and DPPOIPA, and those of the blank epoxy resins (EV and EVP) are displayed in Figs. S4 and S5. The formation of ester bonds causes the merging into a single band of C═O stretching bands of CA and DPPOIPA, centered at 1740 cm^{-1} in EV and around 1714 cm^{-1} in EVP, respectively, in agreement with reports on DGEBA crosslinked with carboxylic acids [54,57]. In EVP (Fig. 3a), this band appears broader and red-shifted due to the coexistence of citrate and isophthalate groups. The successful introduction of DPPOIPA into the polymer network is testified by the presence of the characteristic vibrational bands of triphenylphosphine oxide in EVP, particularly the band at 1436 cm^{-1}, assigned to the C═C stretching in the phenyl rings, the two overlapped bands around 1170 cm^{-1}, arising from P═O stretching and C–H bending, the one at 1118 cm^{-1} (a vibration involving P–C stretching) and the group of bands below 800 cm^{-1} [58,59]. ICP analysis further confirms the incorporation of DPPOIPA, indicating a P content of approximately 2 wt %, which is close to the nominal value (Table 1).

The FTIR spectra of the EVP set of samples are displayed in Fig. 3a. All the spectra are normalized with respect to the strong absorption bands at 1508 cm^{-1}, related to the C═C bonds of the bisphenol rings, which are not expected to be altered during the curing process [54]. The completeness of the cure can be verified by the disappearance of the stretching band of oxirane rings at 914 cm^{-1} (see the spectrum of DGEBA, Fig. S4), meaning that they have reacted, forming crosslinks [33,60]. This band is still observed in the EV matrix, while it completely vanishes in EVP and EVP-SNP indicating an efficient crosslinking. The spectrum of EVP-SNP is very similar to that of the unfilled EVP, suggesting that SiNbP allows the formation of an extended polyester network without establishing strong chemical interactions with its main functional groups. On the other hand, EVP-SN and EVP-SP show a slightly shifted residual band at 902 cm^{-1} and a splitting of the carbonyl stretching band, with a component at 1690 cm^{-1}, which suggest that some oxirane and carboxylic groups remained unreacted. Finally, it should be noted that in the spectra of composites containing the mixed oxide particles, the features of the silicate framework (reported in Fig. 1a) are partly overlapped with vibrations of the polymer matrix.

Table 2
Glass transition temperature values (determined by DSC on as prepared and recycled samples).

Sample	Tg (°C) (original)	Tg (°C) (recycled)
EVP	120	–
EVP-SN	120	123
EVP-SP	122	124
EVP-SNP	99	101

The glass transition temperature (T_g) of the studied samples was evaluated using the DSC thermograms (Fig. S6), by applying the tangent method on the second heating curve. The results are reported in Tables 2 and S4. Pristine EVP shows a relatively high T_g value of 120 °C, slightly lower than EV (126 °C). The partial substitution of citric acid with DPPOIPA introduces bulky phenyl pendant groups into the polymer chains, making their packing looser and increasing mobility. Indeed, triphenylphosphine oxides and similar aromatic compounds can exert a plasticizing effect in thermosets in addition to their flame retardant action [61]. The addition of SiNb or SiP leaves the T_g of EVP almost unvaried (Table 2). At the same time, it decreases to about 100 °C in EVP-SNP, possibly because phenyl rings negatively interfere by steric hindrance and with the establishment of hydrogen bond interactions between the hydrophilic surface of the particles and the hydroxyl groups on the crosslinked polymer chains. In the case of EV-SNP, the steric hindrance does not occur; thus, its T_g results are slightly higher than that of EV (Table S4). It can also be considered that a detrimental effect on the T_g of the composite might be due to a non-uniform dispersion of the filler.

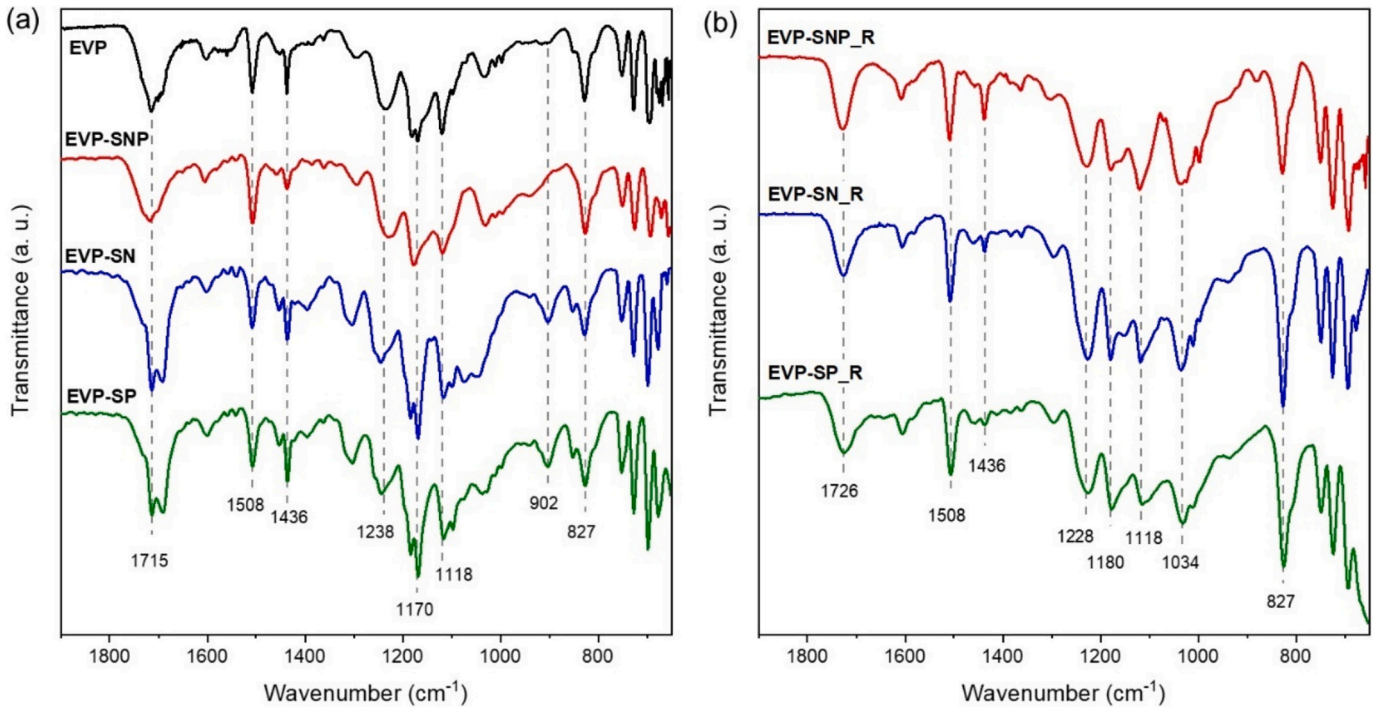

Fig. 3. ATR-FTIR spectra of cured DGEBA-CA-DPPOIPA (EVP) resins (a) as prepared and (b) after thermochemical recycling.

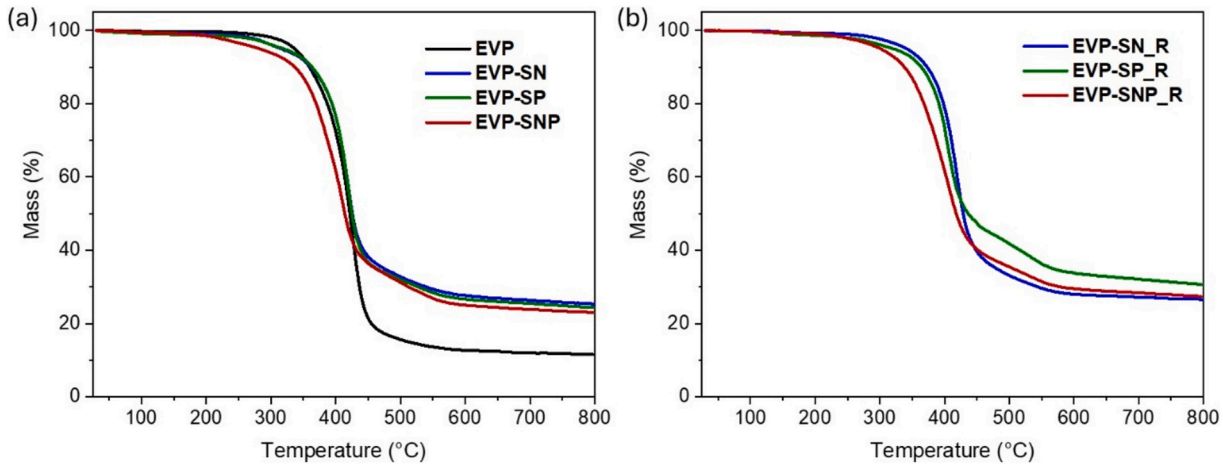

Fig. 4. TGA curves recorded in nitrogen atmosphere: (a) studied epoxy samples of the EVP series; (b) EVP composite samples after reprocessing.

Table 3
TGA data, obtained in a nitrogen atmosphere, of as prepared and recycled EVP samples: the temperature at which 5 % mass loss is observed ($T_{5\%}$), the temperature at which the maximum mass loss rate is observed (T_{max}), and residual masses.

Sample	Original				Recycled			
	$T_{5\%}$ (°C)	T_{max} (°C)	Residue (wt%) at		$T_{5\%}$ (°C)	T_{max} (°C)	Residue (wt%) at	
			T_{max}	800 °C			T_{max}	800 °C
EVP	337	426	44	12	–	–	–	–
EVP-SN	315	418	58	25	340	419	70	26
EVP-SP	318	417	57	24	322	407	67	30
EVP-SNP	284	408	56	23	306	405	58	27

The thermal stability of the epoxy resins was assessed by TGA in an inert atmosphere (Fig. 4a, Table 3). The incorporation of DPPOIPA in EV leads to a notable increase (about 80 °C) of the initial degradation temperature ($T_{5\%}$) (Table S5). A similar effect was found with another modified diphenyl phosphine oxide and attributed to a more extended crosslinking of the resin [31]. Here, the introduction of the functionalized aromatic rings of DPPOIPA in the polymer chains may further benefit the thermal stability in the initial decomposition stage. On the other hand, no significant difference is observed in the residual mass at 800 °C of the two catalyst-free samples. The mixed oxides cause an earlier start of the pyrolytic decomposition of the matrix, giving a drop in the $T_{5\%}$ and T_{max} values with respect to EVP. This decrease can be ascribed to their acidic characteristics, which promote dehydration and degradation reactions. However, it appears less evident in the case of SiNb and SiP, likely ascribed to a milder effect of their surface acidity on the thermal decomposition profiles. In the absence of DPPOIPA, the three mixed oxides show similar effectiveness in preserving the thermal stability of the polymer network, as attested by the $T_{5\%}$ and T_{max} values (Fig. S7, Table S5). The final residue doubles in the presence of the catalysts in the EVP matrix, as also observed in EV-SNP. The solid acids seemingly support char formation during pyrolytic decomposition, especially in the EVP systems, whose thermal degradation leads to the generation of acidic phosphorus compounds that contribute to the charring effect [30]. These results could suggest a condensed phase action exerted by the phosphorus-containing moieties in synergy with the mixed oxides, allowing the production of a more stable char with a significant ceramic content.

3.4. Reprocessability of the epoxy-based vitrimers

The recyclability of the prepared materials was tested through a thermomechanical process, by hot-pressing the powders as described in the Experimental. The driving force of the reprocessing is constituted by the dynamic bond exchanges, namely the transesterification reactions. A first visual inspection of the materials after reprocessing hints at the process's effectiveness (Fig. 5a). A temperature of 250 °C was chosen, because the compactness and homogeneity of some samples reprocessed at lower temperatures was unsatisfactory. Submitting unfilled EV and EVP to the same reprocessing cycle, it was not possible to obtain samples showing a continuous and coherent structure (especially on the edge areas), confirming the crucial role of the catalysts in enabling good recyclability. The recycled samples of the EV set, filled by mixed oxides, exhibited several partly unreacted zones that appeared as powder aggregates toward the outer edge of the ring plate (Fig. 5a). On the other hand, better results were generally observed in the case of samples containing DPPOIPA, especially EVP-SP, which appeared as more homogeneous plates with only slight incompletely fused powder on the edge areas (Fig. 5a). Therefore, the analysis of the recycled materials was focused on the EVP set. Their better reprocessability demonstrates that the presence of the DPPOIPA units in the network positively affects its topological rearrangement by dynamic bond exchanges. The apparently enhanced reactivity to transesterification might be related to electronic or steric reasons, for example, an easier nucleophilic substitution on the carbonyl groups in the isophthalate moiety of DPPOIPA or a higher availability of the carbonyls in the planar isophthalate structure than those in the branched citrate moiety.

To explore the recycling mechanism, rheological stress relaxation experiments were carried out on the samples showing the best recyclability attitude: EV-SP and EVP-SP. These experiments assess how efficiently the materials dissipate stress after deformation, which is driven by heat-triggered network rearrangement in vitrimers [62]. The curves show stress relaxation (σ/σ_0) over time at different temperatures (Fig. 5b and c). As the temperature increases, the relaxation occurs faster. This is expected since higher temperatures generally increase molecular mobility and accelerate the dynamic bond exchange processes in vitrimers or polymers with a covalent adaptable network. The curves are generally stretched over time, indicating a broad distribution of relaxation times. This behavior is typical of vitrimers, whose stress relaxation

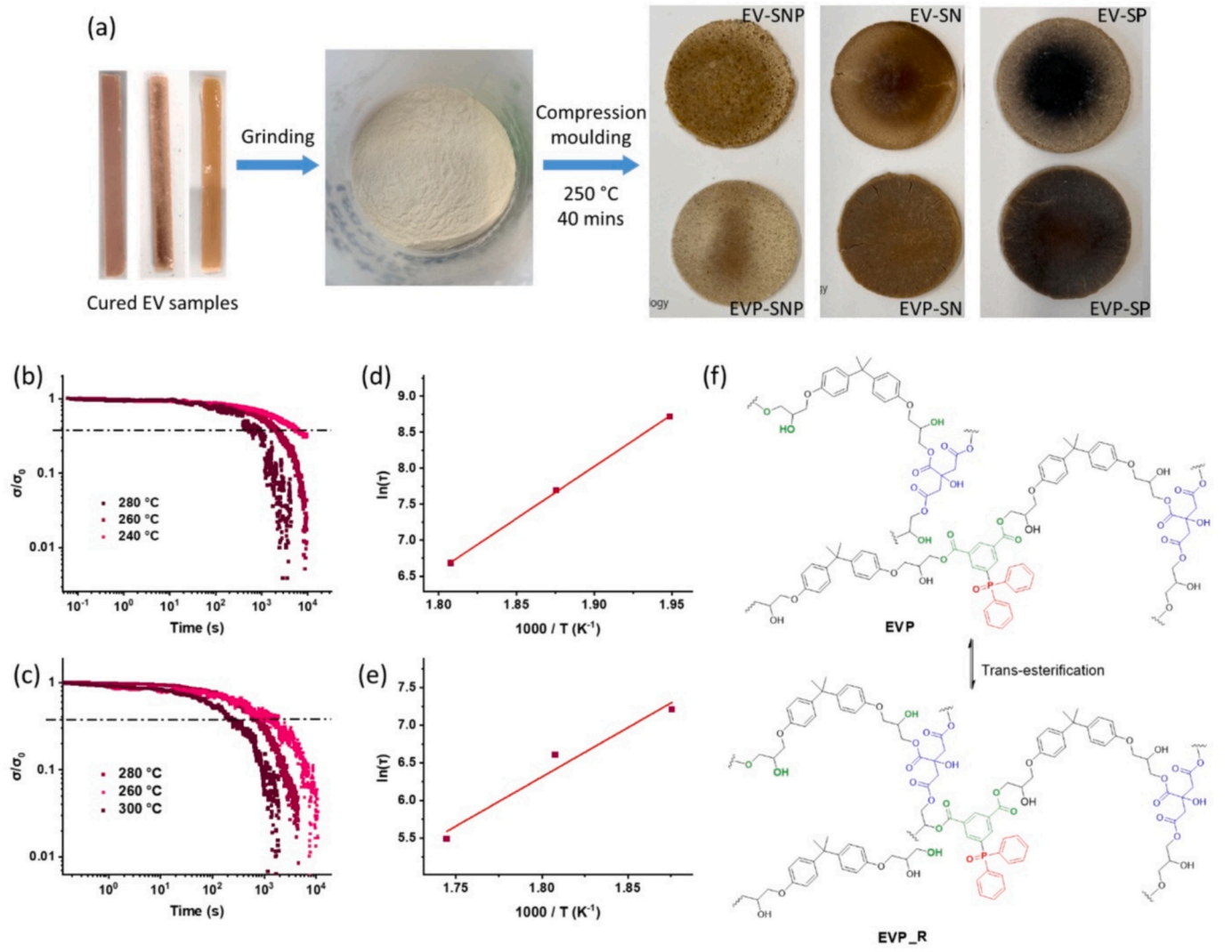

Fig. 5. (a) Streamlined overview of the recycling process via a grinding and moulding procedure, (b) and (c) stress relaxation curves of the EV-SP and EVP-SP samples, (d) and (e) the corresponding Arrhenius plots indicating the temperature dependence of relaxation times, and (f) the predicted transesterification mechanism that allows to switch between different topological arrangements (EVP and EVP_R).

follows a stretched exponential model in a range of relaxation times [63]. The resulting Arrhenius plots display the logarithm of the characteristic relaxation time (τ) against the inverse of temperature (1/T). The fitted lines in Fig. 5d and e suggest that the relaxation times reflect an Arrhenius-type behavior. The linearity of these plots indicates that a thermally activated process governs the material's relaxation. Indeed, the slopes of lines referred to EV-SP and EVP-SP (Fig. 5d and e) correspond to the activation energies for the bond exchange processes (Fig. 5f). The steeper slope in EV-SP implies a higher activation energy ($E_a = 120.0$ kJ/mol) for the relaxation process at the tested temperatures (240–280 °C), as compared with EVP-SP, which is characterized by a slightly lower activation energy ($E_a = 108.7$ kJ/mol) for the 260–300 °C range.

The possible chemical modifications occurring during the recycling tests were investigated by ATR-FTIR spectroscopy (Fig. 3b). The spectrum of EVP-SNP_R reveals that its chemical structure remained substantially unaltered, as no evident changes in any of its characteristic vibrational bands are seen. On the other hand, EVP-SP_R and EVP-SN_R show more significant modifications of the IR spectra. The trace of oxirane rings disappeared, and the C═O stretching band of the ester groups appears unchanged, indicating a virtually complete crosslinking of the matrix. At the same time, some changes in relative intensities can be seen, involving the band at 1436 cm^{-1} and those between 1228 and 1034 cm^{-1}. In particular, the latter two bands, related to C–O bonds [33], tend to grow in intensity, suggesting that a slight oxidative degradation of the polymer matrix occurs during reprocessing. The DSC curves of reprocessed EVP composites, shown in Fig. S6, reveal that their T_g values (Table 2) remain almost unvaried. These data indicate that the crosslinking density is mainly preserved after the topological rearrangement occurring during transesterification reactions, supporting an associative mechanism of dynamic bond exchange. As can be observed from TGA data in Fig. 4b and Table 3, physical recycling causes a delay in the initial decomposition of the materials, though the increase in $T_{5\%}$ values can also be related to the removal of some volatile species, and it results in higher residual masses as compared to original samples. Overall, thermal stability appears enhanced after reprocessing, suggesting that well-crosslinked networks are obtained.

Based on these results, the mixed oxides act as effective catalysts for recycling the epoxy vitrimers containing phosphorus-based moieties, allowing them to maintain their chemical structure, glass transition temperature, and thermal properties. These performances are associated with favorable acid site strength and distribution (Section 3.1). In particular, the efficiency of SiP suggests that a pronounced Brønsted acidity is suitable to promote transesterification in the polyester

network, in line with previous studies dealing with homogeneous acid catalysts [39,40]. Considering the effectiveness of gel-derived oxides in enabling the recyclability of vitrimers, these materials may represent a valuable alternative to commercial catalysts for transesterification reactions, such as $Zn(OAc)_2$ [31]. Furthermore, their chemical characteristics not only induce charring of the polymer matrix during its decomposition, revealing their possible role in enhancing the flame retardancy, but also prevent eventual degradation that may occur in the case of the catalysts containing an organic component employed in high-temperature thermomechanical recycling processes.

Finally, chemical stability tests were conducted in both polar and non-polar solvents to assess the chemical resistance of phosphine oxide epoxy-based vitrimers under thermal stress. The service life of a flame retardant P-based epoxy vitrimer, as well as its efficiency in terms of recyclability and flame retardancy, is strongly affected by the leaching of phosphorus, which usually occurs as a consequence of the degradation of the P-moieties. Table S6 shows that EVP-SP retains more phosphorus after extraction in both chloroform and water compared to the catalyst-free sample EVP. Specifically, EVP-SP retained 81 % of its phosphorus content after chloroform extraction and 95 % after water extraction, while EVP retained only 75 % and 87 %, respectively. These results demonstrate that the presence of SiP ensures the efficient binding of phosphorus units to the matrix, making vitrimers less sensitive to hydrolysis and organic solvents. This indicates that the diphenylphosphoryl units of DPPOIPA are preserved in both polar and non-polar environments.

3.5. Fire behavior of the epoxy-based vitrimers

To assess the flammability of all samples and investigate more deeply the effects of the incorporation of phenyl phosphine oxide pendant groups in the epoxy network, the UL 94 vertical burning test was performed by following the standard procedure [64]. The pristine systems (EV), even including acid catalysts (EV-SNP, EV-SP, EV-SN), could not be classified according to the UL 94 requirements (Table 4), as the flame application resulted in a complete consumption of the material. However, EV-SP exhibited no dripping phenomena, probably due to the acidic characteristics of SiP (see Section 3.1), leading to a significant increase in the viscosity of the burning system during the flammability test and the consequent formation of a continuous char [65,66]. Conversely, the embedding of phosphine oxide moieties in the epoxy network (EVP), combined with the use of catalysts (EVP-SN, EVP-SP, EVP-SNP), lowers the flammability of the final products (Table 4). All the epoxy polyesters containing DPPOIPA showed self-extinguishing behavior and no dripping V-0 rating.

The presence of phosphine oxide units may be responsible for an inhibition effect exerted by phosphorus radicals formed through the decomposition of DPPOIPA moieties in the gas phase [67,68]. For samples filled by mixed oxides, the acid catalysts may additionally dehydrate the polymer matrix and boost the production of residual char able to act as a heat barrier, limiting the generation of combustible volatiles and thus the start of the flaming combustion.

Table 4
UL 94 vertical burning test results for all the investigated samples.

Sample	UL 94/dripping
EV	NC*/YES
EVP	V-0/NO
EV-SN	NC/YES
EVP-SN	V-0/NO
EV-SP	NC/NO
EVP-SP	V-0/NO
EV-SNP	NC/YES
EVP-SNP	V-0/NO

* NC = not classifiable.

Pyrolysis combustion flow calorimetry (PCFC) tests were carried out to shed light on the flame retardant mechanisms during the combustion of the studied epoxy vitrimers. PCFC is a non-flaming calorimetry test and involves controlled pyrolysis of specimens under an inert gas stream, followed by oxidation at high temperatures of the volatiles in a separate chamber [69,70]. Thus, the heat release is measured from the oxygen consumption in pyrolysis conditions. In Table S7, the main parameters of PCFC tests are reported. It is noted that the addition of the catalysts into EV or EVP causes a slight increase in the residue. This effect is even more relevant for samples modified by DPPOIPA and containing the acid solids, whose THR values are lower than the ones of blank EV and EVP (Table S7). The superior acidic characteristics of the catalysts significantly promote the charring of the polymer matrix, leading to the production of more carbonaceous material, where the decomposition of P derivatives and ester moieties contributes to this phenomenon. Table S7 shows that in the case of blank EVP, the residual mass, the pHRR and the THR were ~1.4 %, ~376 W/g and ~25 kJ/g. Especially the addition of SiNbP into EVP is responsible for a decrease of the pHRR and THR by around 36 % and 24 %, respectively, together with an increase of the residue up to 5.1 %. The above flame retardant mechanisms and the lower fuel concentration contained in EVP-SNP may explain its different fire behavior compared to EV [31].

Cone calorimetry (CC) tests were performed to investigate further the effect arising from the incorporation of DPPOIPA and different catalysts on the fire performances of epoxy polyesters. With respect to the EV set (Fig. 6a), the HRR curves of the EVP formulations (Fig. 6b) appear broader and flattened, revealing that the presence of DPPOIPA in the epoxy network results in a relatively slower heat release over a longer timespan [71,72]. Also, the presence of phosphine pendant groups combined with mixed oxides leads to an increase in the Time to Ignition (TTI), particularly noticeable with SiNb, as indicated in Table 5. This may be due to the heat sink effect caused by many ester moieties that endothermically decompose, postponing the ignition phenomena. The combination of acidic characteristics of the mixed oxides and the P derivatives resulting from the decomposition of DPPOIPA cause generally lower THR and pHRR values than the ones of EV-based samples (Table 5). In particular, EVP-SN and EVP-SNP formulations exhibit the lowest pHRR, which decreases up to ~63 % compared to the pristine resin. These results well agree with the ones observed from TGA measurements (see Section 3.3) and suggest a crucial role of Nb and its acidic characteristics (see Section 3.1) in enhancing the thermal stability of the epoxy network. In combination with the charring catalytic effect of P derivatives, the strong acidity of SiNbP may boost the dehydration of the polymer matrix and its carbonization process, forming a stable char that lowers the heat exchange at the boundary phase during the combustion.

SEM images showing the inner structures of chars obtained from CC tests of EVP-SNP, EVP-SP, and EVP-SN are reported in Fig. 6c and d. It is possible to note that the morphology of the char formed by the decomposition of EVP-SNP is the only one free of holes and cracks. EDX analysis (Fig. 6e) indicates that the surface of this ceramic carbonaceous material is fully covered by uniformly distributed Si, P and Nb. The presence of inorganic species and the continuous morphology of the char surface contribute to its effectiveness as a barrier toward heat and oxygen during combustion.

Noticeably, the incorporation of mixed oxides into either a pristine epoxy system or one modified by phenyl phosphine oxide groups suppresses the TSR (up to 62 %) and SEA (up to 71 %) parameters during the CC tests (see Table 6), possibly due to their porous ceramic structure. This smoke suppressant aspect is highly desirable in fire safety science, as smoke often kills both the people escaping and the firemen during work.

Table 6 shows that adding DPPOIPA, especially in combination with mixed oxides, into the epoxy matrix increases CO/CO_2 values, which is particularly relevant with Nb-containing oxides. It seems that the presence of the mixed oxides in the polymer matrix boosts the release of the phosphorus radicals formed by the decomposition of DPPOIPA and,

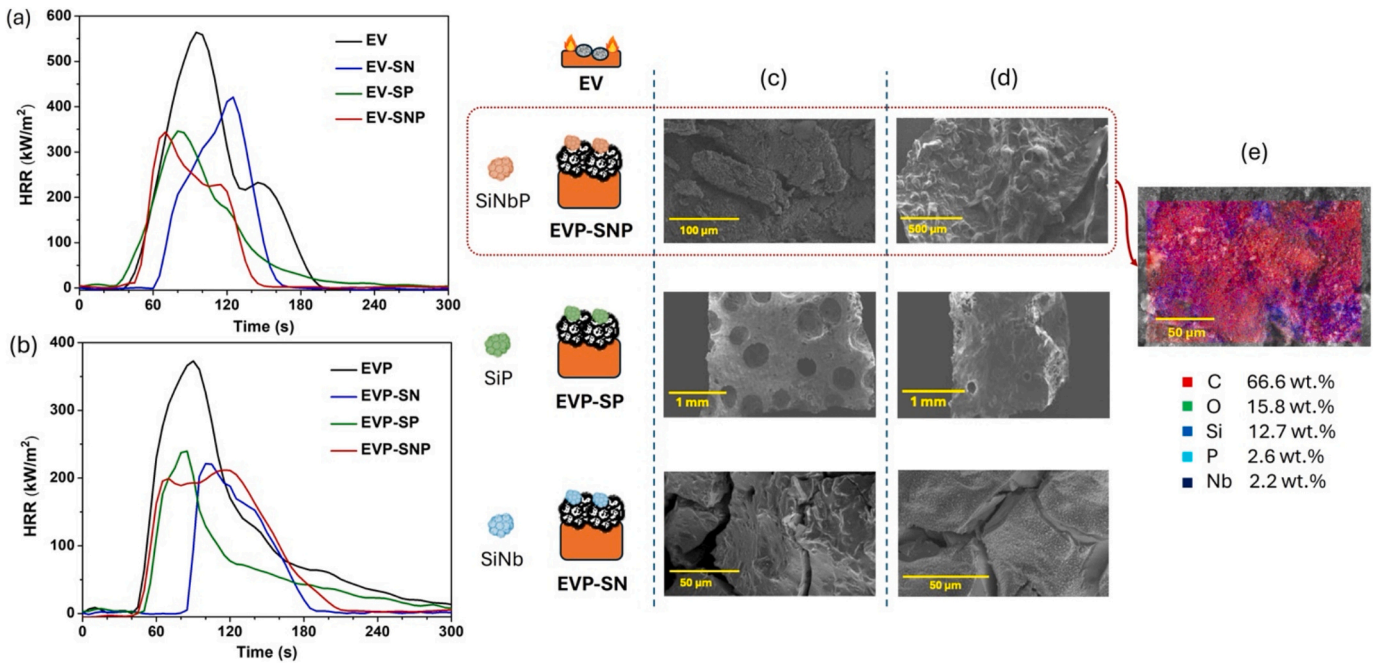

Fig. 6. Heat release rate curves obtained by CC for (a) EV and (b) EVP samples. Scheme of flame retardant mechanisms taking place in the condensed phase during the combustion of EVP-SNP, EVP-SP, and EVP-SN; SEM images of residual chars from CC tests showing the morphology of (c) inner and (d) external structures; (e) SEM-EDX map of residual char from EVP-SNP with corresponding element mass abundance.

Table 5
Cone calorimetry data overview for all the investigated samples.

Sample	TTI (s)	TTFO (s)	THR (MJ/m^2)	MLR ($g/s{\cdot}m^2$)	pHRR (kW/m^2)
EV	31 ± 4	197 ± 18	40 ± 1	8 ± 2	573 ± 5
EVP	36 ± 1	286 ± 23	36 ± 2	5 ± 1	390 ± 73
EV-SN	75 ± 20	165 ± 18	23 ± 2	19 ± 2	440 ± 2
EVP-SN	95 ± 12	186 ± 6	14 ± 1	11 ± 6	216 ± 7
EV-SP	41 ± 9	211 ± 26	27 ± 2	11 ± 1	369 ± 34
EVP-SP	54 ± 3	282 ± 10	20 ± 3	3 ± 1	261 ± 8
EV-SNP	52 ± 4	224 ± 27	20 ± 3	14 ± 3	355 ± 3
EVP-SNP	53 ± 1	205 ± 21	25 ± 2	4 ± 1	214 ± 22

TTI = Time To Ignition, **TTFO** = Time To Flame Out, **THR** = Total Heat Release, **MLR** = Mass Loss Rate, **pHRR** = peak of Heat Release Rate.

thus, the increased inhibition effect in the gas phase [73,74]. This role exerted by the catalysts may additionally explain the lower pHRR values of EVP-SNP, EVP-SP, and EVP-SN compared to the one of EVP (Table 5). It is generally reported that gas phase active phosphorus-based flame retardants cause an increase in TSR values. However, despite the strong gas phase effect, confirmed by the trend of CO/CO_2 values, the presence of mixed oxides considerably reduces the smoke release during the combustion (Table 6).

To confirm the hybrid flame retardant mechanism in the condensed and gas phases exerted by DPPOIPA, and further investigate the role of the catalysts in the fire retardant action, an evolved gas analysis was performed by direct inlet probe mass spectrometry (DIP-MS) for all the prepared samples. Fig. 7a shows the total ion chromatograms from DIP-MS measurements for EV-SNP and EVP-SNP, which reveal that the latter starts to decompose at a very early stage (about 250 °C). However, most volatile species are released above 400 °C, which is related to polymer degradation products. Fig. 7b and c show the relative abundance of PO radical ($m/z = 47$) and diphenyl PO radical (m/z = 201) along time and temperature. The chromatograms corresponding to the other studied materials are reported in Fig. S8. Based on the DIP-MS results (Figs. 7c, S8c and S8f), phosphorus species are released once the P—C bonds in the DPPOIPA moieties break (see Scheme 1). In general, the incorporation of DPPOIPA into the epoxy matrix causes the production of large amounts of P-based radicals. Notably, the samples containing Nb oxides release more radicals (PO and diphenyl) starting from a lower temperature. The P species derived from the degradation of DPPOIPA, namely PO radicals, play a key role in the gas phase, acting as flame inhibitors by the termination of the H• and •OH free radicals in the combustion zone and causing the interruption of the chain reactions related to burning (as shown in Fig. 7d). This agrees well with the higher CO/CO_2 ratios and TSR values observed in CC tests for EVP-based samples with respect to EV (Table 6) [75].

Table 6
Smoke parameters from CC tests for all the investigated samples.

Sample	TSR (m^2/m^2)	SEA (m^2/kg)	CO yield (kg/kg)	CO_2 yield (kg/kg)	CO/CO_2 (–)
EV	1755 ± 9	1858 ± 6	0.2 ± 0.005	4.1 ± 0.05	0.05
EVP	2357 ± 41	2537 ± 26	0.4 ± 0.04	3.0 ± 0.13	0.14
EV-SN	828 ± 17	642 ± 48	0.1 ± 0.01	1.0 ± 0.09	0.10
EVP-SN	993 ± 29	921 ± 17	0.2 ± 0.02	0.6 ± 0.04	0.33
EV-SP	927 ± 46	658 ± 5	0.1 ± 0.01	1.0 ± 0.01	0.08
EVP-SP	877 ± 16	728 ± 38	0.2 ± 0.01	0.9 ± 0.01	0.22
EV-SNP	777 ± 45	727 ± 25	0.1 ± 0.01	1.2 ± 0.05	0.08
EVP-SNP	1306 ± 19	740 ± 6	0.3 ± 0.02	0.8 ± 0.03	0.37

TSR = Total Smoke Release, **SEA** = Smoke Extension Area.

A large amount of PO species from DPPOIPA, together with the decomposition products of the epoxy matrix, is released from EVP-SNP, supporting the very low flammability of this sample. However, SiNb and SiP can also improve the effectiveness of DPPOIPA in its flame retardant action in the gas phase, promoting the release of PO radicals in the early stages of decomposition of the matrix (see Fig. S8). The synergism between DPPOIPA and solid acids explains the very good fire behavior of EVP-SN, EVP-SP, and EVP-SNP compared to EVP and the EV set. From the smoke data of CC, adding DPPOIPA into the polymer matrix increases smoke production and gas phase inhibition activity (increased CO/CO_2 ratio), a typical behavior of phosphorus flame retardants in an epoxy matrix. However, adding the solid catalyst helps reduce smoke production without adversely affecting the gas phase flame inhibition.

These results demonstrate that a mixed oxide with proper acidic

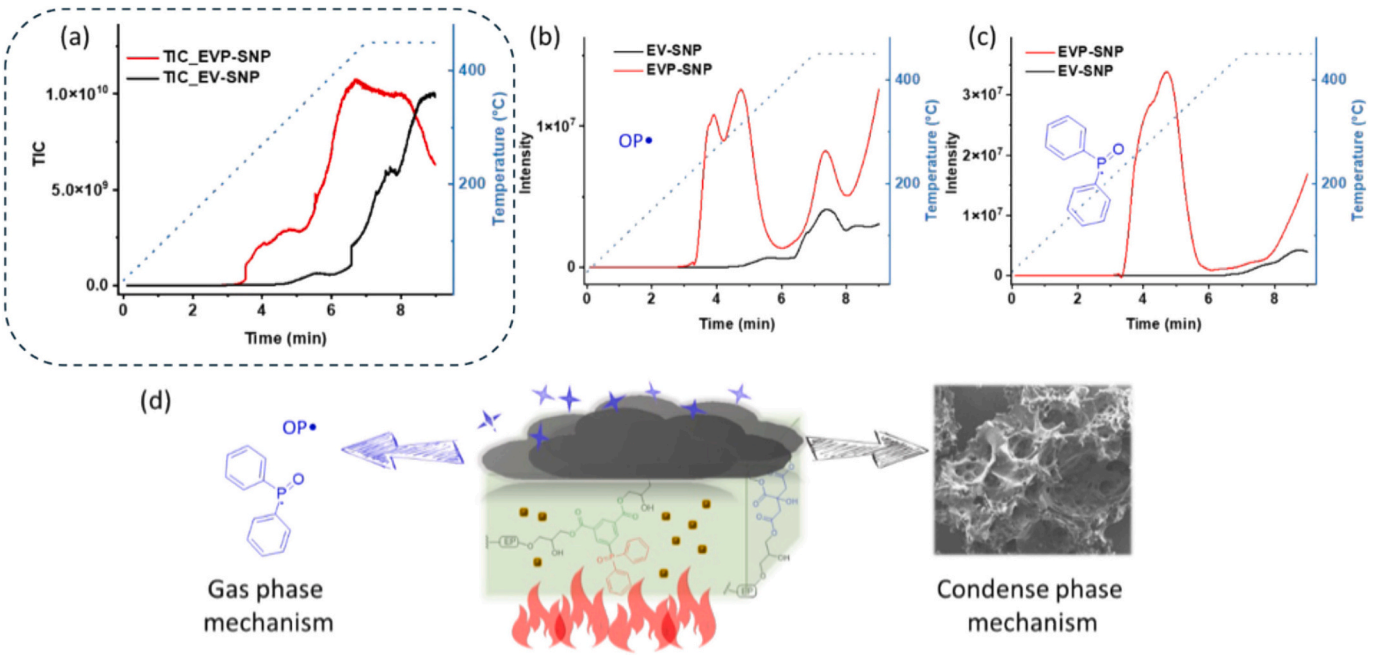

Fig. 7. (a) Total ion chromatograms showing the relative abundance of species produced along the time and temperature during the decomposition of EV-SNP and EVP-SNP from DIP-MS; relative abundance of PO (b) and diphenyl PO (c) radicals identified during the measurements; (d) the proposed flame retardant mechanism exerted by DPPOIPA and catalysts during the combustion.

features and chemical composition can work as a flame retardant synergist, effective smoke suppressant, and transesterification catalyst, allowing the efficient design of no dripping self-extinguishing P-containing epoxy polyesters with satisfactory recyclability and glass transition temperature. These outcomes may help to limit the depletion of natural resources, fostering the future development of inherently flame retardant epoxy vitrimers, whose concentration of P and other precious materials are kept as low as possible by the proper design of new mixed oxides with flame retardant features.

3.6. Performance comparison between epoxy-based vitrimers obtained by using Zn(II) acetate or mixed oxides catalysts

To highlight the difference in terms of performance between the use of Zn(II) acetate and mixed oxides in the preparation of phosphine oxide epoxy-based covalent adaptable networks, additional experiments were also performed on samples (EVP-Zn) containing DPPOIPA and Zn $(OAc)_2$. This comparison allows us to underline the advantages and drawbacks arising from the use of solid acidic catalysts in EVP as an alternative to Zn(II) acetate, which is a common catalyst for transesterification-based CANs [33,76]. The sample free of DPPOIPA and filled by $Zn(OAc)_2$ alone was not taken into account, as the presence of the phosphine oxide is undeniable to obtain excellent flame retardancy and recyclability.

As shown in Table 7, all the catalysts exhibit lower E_a (activation energy of the curing process estimated by Kissinger method) than bare EVP, and the extent of the decrease follows the order: EVP-Zn < EVP-SP < EVP-SN < EVP-SNP (see also Figs. 2 and S9). Mixed oxides appear more effective than $Zn(OAc)_2$ in catalyzing the esterification reactions. Notably, SiNbP exhibits approximately 36 % lower E_a than $Zn(OAc)_2$, which can be attributed to its significant acidity and a suitable combination of Brønsted and Lewis acid sites, promoting, under favorable operating conditions, the topological rearrangement of the dynamic network [77]. Considering the thermal stability of the prepared vitrimers, the pronounced acidity of $Zn(OAc)_2$ strongly accelerates the pyrolytic decomposition of the matrix [78,79], causing a drop in the $T_{5\%}$ values (Fig. S10a, Table 7). This decrease is less pronounced in the case of SiNbP, SiNb and SiP, indicating a milder effect of their surface acidity in promoting dehydration and degradation reactions. After thermomechanical recycling, mixed oxides delay the decomposition of the materials compared to zinc acetate, as confirmed by the $T_{5\%}$ values (Fig. S10b, Table 7). In general, the three mixed oxides positively affect the thermal stability of the polymer network, suggesting that well crosslinked networks are obtained by reprocessing. Similarly to the binary solid acids, the presence of $Zn(OAc)_2$ in EVP leaves the T_g of EVP almost unchanged. However, in the case of recycled samples, the T_g strongly decays in EVP-Zn (Fig. S6). In contrast, it remains virtually unchanged in all composites containing mixed oxides (Table 7), revealing that the solid acidic catalysts appear to mitigate the effects of reprocessing on the regular packing and chain mobility of the polymer

Table 7
Activation energies (curing process), thermal properties, and fire performances (UL 94 vertical burning and cone calorimetry tests) of phosphine oxide epoxy-based vitrimers containing Zn(II) acetate and mixed oxides.

Sample	E_a (kJ/mol)	Original		Recycled		UL 94/drip	TTI (s)	pHRR (kW/m^2)	TSR (m^2/m^2)	CO/CO_2 (—)
		$T_{5\%}$ (°C)	Tg (°C)	$T_{5\%}$ (°C)	Tg (°C)					
EVP	156	337	120	–	–	V-0/NO	36 ± 1	390 ± 73	2357 ± 41	0.14
EVP-Zn	154	230	123	270	82	V-1/NO	30 ± 12	320 ± 21	1523 ± 162	0.22
EVP-SN	131	315	120	340	123	V-0/NO	95 ± 12	216 ± 7	993 ± 29	0.33
EVP-SP	141	318	122	322	124	V-0/NO	54 ± 3	261 ± 8	877 ± 16	0.22
EVP-SNP	100	284	99	306	101	V-0/NO	53 ± 1	214 ± 22	1306 ± 19	0.37

chains. Regarding the recyclability, as previously mentioned (section 3.4), the E_a (determined by stress relaxation tests) for the thermally activated bond exchange process gives 108.7 kJ/mol for EVP-SP, which is in the range of the values generally reported in the literature for transesterification reactions catalyzed by $Zn(OAc)_2$ or $Sn(Oct)_2$ in polyester-based vitrimers [80–83].

In comparing the flammability of the epoxy-based vitrimers, EVP-Zn can only achieve a V-1 classification with no dripping, likely due to the acidic characteristics of $Zn(OAc)_2$, which confer lower thermal stability to the final product and lower flame retardant action in the condensed phase during burning (Table 7). CC tests carried out on CANs reveal that the presence of zinc acetate in EVP leads to a moderate decrease in TTI compared to the one observed for systems containing mixed oxides (Fig. S11, Table 7), in agreement with the earlier pyrolytic decomposition of EVP-Zn observed from TGA measurements. The acidic characteristics of the mixed oxides, in synergy with those of P derivatives (acidic phosphorus compounds) resulting from the decomposition of DPPOIPA, cause lower pHRR values and broader HRR curves than EVP-Zn, hence a slower heat release over a longer timespan. The solid acids promote the dehydration of the polymer matrix and its carbonization, resulting in the formation of a char that acts as an effective thermal shield, slowing down the combustion process. Morphological analysis of char obtained from CC tests of EVP-Zn (Fig. S12) shows that its inner and external structures are full of holes. Thus, this carbonaceous residue is not an effective barrier against heat and oxygen during combustion. This also sheds light on the lower fire performance of EVP-Zn compared to epoxy vitrimers containing solid acids, especially EVP-SNP (see Section 3.5). As previously observed for SiNb, SiP, and SiNbP, the smoke data in Table 7, i.e., the increased CO/CO_2 ratio of EVP-Zn compared to that of EVP, reveal that the addition of $Zn(OAc)_2$ also promotes the gas phase inhibition activity of DPPOIPA along the CC tests. However, unlike solid acids, $Zn(OAc)_2$ only allows for ~35 % reduction of TSR, which is significantly lower than the one (up to 62 %) resulting from the use of mixed oxides. Particularly, SiNbP guarantees a higher CO/CO_2 ratio compared to $Zn(OAc)_2$, when employed as a catalyst in EVP, which means that the ternary oxide is more effective in boosting the inhibition mechanisms in the gas phase, keeping very low smoke production during the combustion of final products.

To conclude, mixed oxides, thanks to their peculiar acidic characteristics, represent a valuable alternative to zinc acetate, as they allow to hit two targets with one arrow, enhancing the recycling performances of epoxy vitrimers and their flame retardancy.

4. Conclusion

This work reveals the dual role of acid solids in a novel epoxy-based polyester vitrimer system, which contains phosphine oxide moieties, as catalysts for the transesterification reaction and as flame retardant synergists. Their introduction into the polyester vitrimer formed by crosslinking epoxy resin with citric acid and a diphenyl phosphine oxide derivative (DPPOIPA) causes a reduction in curing activation energy, which is stronger than that observed in the presence of zinc acetate (the conventional catalyst employed in transesterification-based covalent adaptable networks), and promotes thermomechanical recycling. Uniform reprocessed samples with unvaried T_g compared to the original materials are obtained using solid catalysts, particularly SiP oxide. This behavior is attributed to the significant surface acidity, primarily provided by Brønsted acid sites, as revealed by FTIR spectroscopy of adsorbed basic probes. The use of SiP also enhances the chemical stability of phosphine oxide epoxy-based vitrimers under thermal stress in both polar and non-polar solvents, thereby reducing the leaching of phosphorus released from the degradation of DPPOIPA, whose integrity is crucial for maintaining the good recyclability and flame retardancy of final products throughout their service life.

Furthermore, all DPPOIPA-containing vitrimers with acid solids are self-extinguishing, achieving a V-0 rating in the UL 94 vertical burning test, despite having a low P content of approximately 2 wt%. In particular, for the unmodified epoxy system, the cone calorimetry tests reveal that incorporating SiNbP into the P-modified epoxy system allows for a significant reduction in the peak heat release rate (~63 %) and total heat release (~38 %). Cone calorimetry and SEM-EDX analysis of char residues indicate that the effectiveness of SiNbP in improving flame retardancy may be ascribed to a ceramic and continuous char acting as an oxygen and thermal barrier at the condensed phase during the combustion. However, for all formulations containing an acid catalyst and DPPOIPA, the effect in the condensed phase occurs in synergy with an inhibition effect exerted by phosphorus radicals in the gas phase, as demonstrated by evolved gas analysis and supported by the high CO/CO_2 values. Regardless of DPPOIPA modification, all the mixed oxides notably dwindle the TSR (up to 62 %) and SEA (up to 71 %) parameters during the CC tests, a highly desirable aspect in fire safety science. On the other hand, the incorporation of zinc acetate into DPPOIPA-containing vitrimers reduces the TSR by approximately 35 %.

These encouraging results may open new perspectives on using catalytic nanomaterials to manufacture self-extinguishing flame retardant recyclable thermosets with very low smoke emissions. Finally, properly tuning the surface functionalities of such catalysts may enhance the fire resistance and sustainable features of final products, thereby preventing the exploitation of vast amounts of phosphorus-based flame retardants and precious natural resources.

CRediT authorship contribution statement

Valeria Palumbo: Methodology, Investigation, Data curation. **Wenyu Wu Klingler:** Writing – review & editing, Writing – original draft, Validation, Supervision, Methodology, Investigation, Formal analysis, Data curation, Conceptualization. **Nikita Drigo:** Writing – review & editing, Supervision, Investigation. **Ton Markaj:** Investigation. **Aurelio Bifulco:** Writing – original draft, Validation, Supervision, Formal analysis, Data curation, Conceptualization. **Claudio Imparato:** Writing – original draft, Investigation, Conceptualization. **Alex Imboden:** Investigation, Data curation. **Sandro Lehner:** Writing – review & editing, Investigation, Data curation. **Alessia Arpaia:** Investigation, Data curation. **Elisabetta Finocchio:** Writing – original draft, Investigation. **Antonio Aronne:** Writing – review & editing, Conceptualization. **Sabyasachi Gaan:** Writing – review & editing, Supervision, Resources, Project administration, Methodology, Funding acquisition, Conceptualization.

Declaration of competing interest

The authors declare that they have no known competing financial interests or personal relationships that could have appeared to influence the work reported in this paper.

Acknowledgements

We acknowledge the experimental work carried out by Ms. Carolina Polisi for the preparation of vitrimers, under the supervision of Dr. Wenyu Wu Klingler and Dr. Sabyasachi Gaan in Empa, St. Gallen.

Appendix A. Supplementary data

Supplementary data to this article can be found online at https://doi.org/10.1016/j.susmat.2025.e01477.

Data availability

Data will be made available on request.

References

[1] F. Mazur, A.-H. Pham, R. Chandrawati, Polymer materials as catalysts for medical, environmental, and energy applications, Appl. Mater. Today 35 (2023) 101937.
[2] P. Jagadeesh, M. Puttegowda, O.P. Oladijo, C.W. Lai, S. Gorbatyuk, D. Matykiewicz, et al., A comprehensive review on polymer composites in railway applications, Polym. Compos. 43 (3) (2022) 1238–1251.
[3] A.B. Morgan, The future of flame retardant polymers–unmet needs and likely new approaches, Polym. Rev. 59 (1) (2019) 25–54.
[4] B.W. Liu, H.B. Zhao, Y.Z. Wang, Advanced flame-retardant methods for polymeric materials, Adv. Mater. 34 (46) (2022) 2107905.
[5] Y. Liu, Z. Yu, B. Wang, P. Li, J. Zhu, S. Ma, Closed-loop chemical recycling of thermosetting polymers and their applications: a review, Green Chem. 24 (15) (2022) 5691–5708.
[6] S. Utekar, V.K. Suriya, N. More, A. Rao, Comprehensive study of recycling of thermosetting polymer composites–driving force, challenges and methods, Compos. Part B Eng. 207 (2021) 108596.
[7] A. Bifulco, J. Chen, A. Sekar, W.W. Klingler, A. Gooneie, S. Gaan, Recycling of flame retardant polymers: current technologies and future perspectives, J. Mater. Sci. Technol. 199 (2024) 156–183.
[8] J. Wang, J. Wang, S. Yang, C. Wu, X. Chen, K. Chen, et al., Development of single-component epoxy resin with superb thermal stability, flame retardancy, smoke suppression, and latency via Cu-based phosphorus/imidazole-containing complex, Polym. Degrad. Stab. 228 (2024) 110906.
[9] S.-H. Tan, J.-H. He, Y.-F. Xiao, Y.-Z. Wang, L. Chen, Trinity-cooperative flame-retardant strategy towards low flammability of epoxy resin: phosphonate, imine and benzimidazolone, Polym. Degrad. Stab. 234 (2025) 111241.
[10] Y. Luo, Y. Lan, J. Cai, Q. Jiang, X. Wang, H. Zhang, et al., Multi-functional bio-based DOPO derivative for enhanced flame retardancy and mechanical strength in epoxy resin, Eur. Polym. J. 222 (2025) 113605.
[11] H. Vahabi, R. Sonnier, L. Ferry, Effects of ageing on the fire behaviour of flame-retarded polymers: a review, Polym. Int. 64 (3) (2015) 313–328.
[12] C.-D. Varganici, L. Rosu, A. Bifulco, D. Rosu, F. Mustata, S. Gaan, Recent advances in flame retardant epoxy systems from reactive DOPO–based phosphorus additives, Polym. Degrad. Stab. 202 (2022) 110020.
[13] X.-F. Liu, Y.-F. Xiao, X. Luo, B.-W. Liu, D.-M. Guo, L. Chen, et al., Flame-retardant multifunctional epoxy resin with high performances, Chem. Eng. J. 427 (2022) 132031.
[14] C. Ma, Z. Guo, Z. Fang, J. Li, Flame retardancy and chemical degradation of epoxy containing phenylphosphonate group under mild conditions, Compos. Part B Eng. 239 (2022) 109967.
[15] M. Guerre, C. Taplan, J.M. Winne, F.E. Du Prez, Vitrimers: directing chemical reactivity to control material properties, Chem. Sci. 11 (19) (2020) 4855–4870.
[16] C. Bowman, F. Du Prez, J. Kalow, Introduction to chemistry for covalent adaptable networks, Polym. Chem. 11 (33) (2020) 5295–5296.
[17] B. Krishnakumar, R.V.S.P. Sanka, W.H. Binder, V. Parthasarthy, S. Rana, N. Karak, Vitrimers: associative dynamic covalent adaptive networks in thermoset polymers, Chem. Eng. J. 385 (2020) 123820.
[18] M.A. Lucherelli, A. Duval, L. Avérous, Biobased vitrimers: towards sustainable and adaptable performing polymer materials, Prog. Polym. Sci. 127 (2022) 101515.
[19] M. Podgórski, B.D. Fairbanks, B.E. Kirkpatrick, M. McBride, A. Martinez, A. Dobson, et al., Toward stimuli-responsive dynamic thermosets through continuous development and improvements in covalent adaptable networks (CANs), Adv. Mater. 32 (20) (2020) 1906876.
[20] H. Si, L. Zhou, Y. Wu, L. Song, M. Kang, X. Zhao, et al., Rapidly reprocessable, degradable epoxy vitrimer and recyclable carbon fiber reinforced thermoset composites relied on high contents of exchangeable aromatic disulfide crosslinks, Compos. Part B Eng. 199 (2020) 108278.
[21] M. Röttger, T. Domenech, R. van der Weegen, A. Breuillac, R. Nicolaÿ, L. Leibler, High-performance vitrimers from commodity thermoplastics through dioxaborolane metathesis, Science 356 (6333) (2017) 62–65.
[22] Y. Xu, S. Dai, L. Bi, J. Jiang, H. Zhang, Y. Chen, Catalyst-free self-healing bio-based vitrimer for a recyclable, reprocessable, and self-adhered carbon fiber reinforced composite, Chem. Eng. J. 429 (2022) 132518.
[23] X. Liu, E. Zhang, Z. Feng, J. Liu, B. Chen, L. Liang, Degradable bio-based epoxy vitrimers based on imine chemistry and their application in recyclable carbon fiber composites, J. Mater. Sci. 56 (2021) 15733–15751.
[24] X. Feng, G. Li, Catalyst-free β-hydroxy phosphate ester exchange for robust fire-proof vitrimers, Chem. Eng. J. 417 (2021) 129132.
[25] W.W. Klingler, A. Bifulco, C. Polisi, Z. Huang, S. Gaan, Recyclable inherently flame-retardant thermosets: chemistry, properties and applications, Compos. Part B Eng. 258 (2023) 110667.
[26] C. Imparato, A. Bifulco, G. Malucelli, A. Aronne, Solids containing Si-O-P bonds: is the hydrolytic sol-gel route a suitable synthesis strategy? J. Sol-Gel Sci. Technol. (2023) 1–26.
[27] P.A. Turhanen, K.D. Demadis, P. Kafarski, Phosphonate chemistry in drug design and development, Front. Chem. 9 (2021) 695128.
[28] G.P. Horsman, D.L. Zechel, Phosphonate biochemistry, Chem. Rev. 117 (8) (2017) 5704–5783.
[29] M. Spontón, J.C. Ronda, M. Galia, V. Cádiz, Flame retardant epoxy resins based on diglycidyl ether of (2, 5-dihydroxyphenyl) diphenyl phosphine oxide, J. Polym. Sci. A Polym. Chem. 45 (11) (2007) 2142–2151.
[30] W.W. Klingler, V. Rougier, Z. Huang, D. Parida, S. Lehner, A. Casutt, et al., Recyclable flame retardant phosphonated epoxy based thermosets enabled via a reactive approach, Chem. Eng. J. 466 (2023) 143051.
[31] Z. Huang, W.W. Klingler, D. Roncucci, C. Polisi, V. Rougier, S. Lehner, et al., Enabling simultaneous reprocessability and fire protection via incorporation of phosphine oxide monomer in epoxy vitrimer, J. Mater. Sci. Technol. 196 (2024) 224–236.
[32] S. Bhusal, C. Oh, Y. Kang, V. Varshney, Y. Ren, D. Nepal, et al., Transesterification in vitrimer polymers using bifunctional catalysts: modeled with solution-phase experimental rates and theoretical analysis of efficiency and mechanisms, J. Phys. Chem. B 125 (9) (2021) 2411–2424.
[33] A. Demongeot, S.J. Mougnier, S. Okada, C. Soulié-Ziakovic, F. Tournilhac, Coordination and catalysis of Zn^{2+} in epoxy-based vitrimers, Polym. Chem. 7 (27) (2016) 4486–4493.
[34] C. Brondi, A. Marotta, G. Filippone, G. Mensitieri, M. Salzano de Luna, V. Ambrogi, Curing behavior of reprocessable epoxy vitrimers: thermal analysis and kinetics modeling, Macromol. Chem. Phys. 224 (22) (2023) 2300273.
[35] W. Cai, Y. Huang, J. Li, G. Yang, F. Wang, G. Si, et al., A multifunctional biomass zinc catalyst for epoxy-based vitrimers and composites, Eur. Polym. J. 188 (2023) 111936.
[36] B. Palmieri, F. Cilento, E. Amendola, T. Valente, S. Dello Iacono, M. Giordano, et al., Influence of catalyst content and epoxy/carboxylate ratio on isothermal creep of epoxy vitrimers, Polymers 15 (18) (2023) 3845.
[37] X. Niu, F. Wang, X. Li, R. Zhang, Q. Wu, P. Sun, Using Zn^{2+} ionomer to catalyze transesterification reaction in epoxy vitrimer, Ind. Eng. Chem. Res. 58 (14) (2019) 5698–5706.
[38] G. Rizzo, L. Saitta, S. Dattilo, C. Tosto, E. Pergolizzi, A. Ivankovic, et al., Thermomechanical characterization of an unsaturated polyester vitrimer synthesized using a titanium transesterification catalyst, ACS Appl. Polym. Mater. 5 (10) (2023) 8326–8338.
[39] J.L. Self, N.D. Dolinski, M.S. Zayas, J. Read de Alaniz, C.M. Bates, Brønsted-acid-catalyzed exchange in polyester dynamic covalent networks, ACS Macro Lett. 7 (7) (2018) 817–821.
[40] B. Thangaraj, P.R. Solomon, B. Muniyandi, S. Ranganathan, L. Lin, Catalysis in biodiesel production—a review, Clean Energy 3 (1) (2019) 2–23.
[41] N.J. Clayden, C. Imparato, R. Avolio, G. Ferraro, M.E. Errico, A. Vergara, et al., Chloride-free hydrolytic sol-gel synthesis of Nb-P-Si oxides: an approach to solid acid materials, Green Chem. 22 (20) (2020) 7140–7151.
[42] G. Garbarino, G. Pampararo, E. Finocchio, G. Busca, A. Gervasini, S. Campisi, et al., Surface acid properties of Nb_2O_5–P_2O_5–SiO_2 gel-derived catalysts, Microporous Mesoporous Mater. 343 (2022) 112190.
[43] A. Aronne, M. Di Serio, R. Vitiello, N.J. Clayden, L. Minieri, C. Imparato, et al., An environmentally friendly Nb–P–Si solid catalyst for acid-demanding reactions, J. Phys. Chem. C 121 (32) (2017) 17378–17389.
[44] W. Yang, H. Ding, W. Zhou, T. Liu, P. Xu, D. Puglia, et al., Design of inherent fire retarding and degradable bio-based epoxy vitrimer with excellent self-healing and mechanical reprocessability, Compos. Sci. Technol. 230 (2022) 109776.
[45] X.-M. Ding, L. Chen, Y.-J. Xu, X.-H. Shi, X. Luo, X. Song, et al., Robust epoxy vitrimer with simultaneous ultrahigh impact property, fire safety, and multipath recyclability via rigid-flexible imine networks, ACS Sustain. Chem. Eng. 11 (39) (2023) 14445–14456.
[46] E. Finocchio, C. Cristiani, G. Dotelli, P.G. Stampino, L. Zampori, Thermal evolution of PEG-based and BRIJ-based hybrid organo-inorganic materials. FT-IR studies, Vibr. Spectrosc. 71 (2014) 47–56.
[47] H.E. Kissinger, Reaction kinetics in differential thermal analysis, Anal. Chem. 29 (11) (1957) 1702–1706.
[48] L. Yu, X. Sun, Y. Jin, W. Zhang, R. Long, Mechanics of vitrimer particle compression and fusion under heat press, Int. J. Mech. Sci. 201 (2021) 106466.
[49] D. Liu, X. Niu, Z. Guo, K. Zhang, N. Jiang, Y. Qin, et al., One-pot solvent-free sequential synthesis of high-density polycycloalkanes fuels from lignin-derivatives over laminated $NbOPO_4$ catalyst, Fuel 360 (2024) 130570.
[50] Y. Huang, Q. Li, A.H. Jensen, M. Yin, J.O. Jensen, E. Christensen, et al., Niobium phosphates as an intermediate temperature proton conducting electrolyte for fuel cells, J. Mater. Chem. 22 (42) (2012) 22452–22458.
[51] P. Carniti, A. Gervasini, F. Bossola, V. Dal Santo, Cooperative action of Brønsted and Lewis acid sites of niobium phosphate catalysts for cellobiose conversion in water, Appl. Catal. Environ. 193 (2016) 93–102.
[52] G. Busca, The surface acidity of solid oxides and its characterization by IR spectroscopic methods. An attempt at systematization, Phys. Chem. Chem. Phys. 1 (5) (1999) 723–736.
[53] C. Imparato, E. Finocchio, S. Campisi, M. Bigica, A. Gervasini, A. Bifulco, R. Avolio, N.J. Clayden, M.E. Errico, A. Aronne, Insight into titanium and zirconium phosphate-based materials for reactive surfaces, Mater. Today Chem. 38 (2024) 102126.
[54] Q.-A. Poutrel, J.J. Blaker, C. Soutis, F. Tournilhac, M. Gresil, Dicarboxylic acid-epoxy vitrimers: influence of the off-stoichiometric acid content on cure reactions and thermo-mechanical properties, Polym. Chem. 11 (33) (2020) 5327–5338.
[55] S. Vyazovkin, A.K. Burnham, J.M. Criado, L.A. Pérez-Maqueda, C. Popescu, N. Sbirrazzuoli, ICTAC kinetics committee recommendations for performing kinetic computations on thermal analysis data, Thermochim. Acta 520 (1–2) (2011) 1–19.
[56] R. Hardis, J.L.P. Jessop, F.E. Peters, M.R. Kessler, Cure kinetics characterization and monitoring of an epoxy resin using DSC, Raman spectroscopy, and DEA, Compos. A: Appl. Sci. Manuf. 49 (2013) 100–108.
[57] E. Manarin, F. Da Via, B. Rigatelli, S. Turri, G. Griffini, Bio-based vitrimers from 2, 5-furandicarboxylic acid as repairable, reusable, and recyclable epoxy systems, ACS Appl. Polym. Mater. 5 (1) (2022) 828–838.

[58] G.B. Deacon, J.H.S. Green, Vibrational spectra of ligands and complexes—II infrared spectra (3650–375 cm^{-1}) of triphenyl-phosphine, triphenylphosphine oxide, and their complexes, Spectrochim. Acta A: Mol. Spectrosc. 24 (7) (1968) 845–852.
[59] C. Ma, L. Qian, Z. Guo, J. Li, Self-compatibilization effect of phosphonate with cyano group on flame retardancy and mechanical properties of epoxy, Polymer 234 (2021) 124236.
[60] S. Kocaman, G. Ahmetli, A study of coating properties of biobased modified epoxy resin with different hardeners, Prog. Org. Coat. 97 (2016) 53–64.
[61] A. Battig, P. Müller, A. Bertin, B. Schartel, Hyperbranched rigid aromatic phosphorus-containing flame retardants for epoxy resins, Macromol. Mater. Eng. 306 (4) (2021) 2000731.
[62] H. Fang, W. Ye, Y. Ding, H.H. Winter, Rheology of the critical transition state of an epoxy vitrimer, Macromolecules 53 (12) (2020) 4855–4862.
[63] F. Meng, M.O. Saed, E.M. Terentjev, Rheology of vitrimers, Nat. Commun. 13 (1) (2022) 5753.
[64] A.B. Morgan, M. Bundy, Cone calorimeter analysis of UL-94 V-rated plastics, Fire Mater. 31 (4) (2007) 257–283.
[65] T. Kashiwagi, J.W. Gilman, K.M. Butler, R.H. Harris, J.R. Shields, A. Asano, Flame retardant mechanism of silica gel/silica, Fire Mater. 24 (6) (2000) 277–289.
[66] J.W. Gilman, R.H. Harris Jr., J.R. Shields, T. Kashiwagi, A.B. Morgan, A study of the flammability reduction mechanism of polystyrene-layered silicate nanocomposite: layered silicate reinforced carbonaceous char, Polym. Adv. Technol. 17 (4) (2006) 263–271.
[67] H.T. Kreissl, M.M.J. Li, Y.-K. Peng, K. Nakagawa, T.J.N. Hooper, J.V. Hanna, et al., Structural studies of bulk to nanosize niobium oxides with correlation to their acidity, J. Am. Chem. Soc. 139 (36) (2017) 12670–12680.
[68] J.C. Vedrine, G. Coudurier, A. Ouqour, P.G.P. De Oliveira, J.C. Volta, Niobium oxide based materials as catalysts for acidic and partial oxidation type reactions, Catal. Today 28 (1–2) (1996) 3–15.
[69] F. Cuminet, N. Vanachte, C. Farina, M. Denis, C. Negrell, S. Caillol, et al., Phosphorus acid: an asset for flame-retardant sustainable vitrimers, Polym. Chem. 15 (12) (2024) 1212–1226.
[70] R.E. Lyon, R.N. Walters, Pyrolysis combustion flow calorimetry, J. Anal. Appl. Pyrolysis 71 (1) (2004) 27–46.
[71] S. Huo, P. Song, B. Yu, S. Ran, V.S. Chevali, L. Liu, et al., Phosphorus-containing flame retardant epoxy thermosets: recent advances and future perspectives, Prog. Polym. Sci. 114 (2021) 101366.
[72] A. Bifulco, D. Parida, K.A. Salmeia, R. Nazir, S. Lehner, R. Stämpfli, et al., Fire and mechanical properties of DGEBA-based epoxy resin cured with a cycloaliphatic hardener: combined action of silica, melamine and DOPO-derivative, Mater. Des. 193 (2020) 108862.
[73] K. Salmeia, J. Fage, S. Liang, S. Gaan, An overview of mode of action and analytical methods for evaluation of gas phase activities of flame retardants, Polymers 7 (3) (2015) 504–526.
[74] A. Lamandé, V. Marchetti, S. Bourbigot, G. Fontaine, Effects of oxygen concentration on the reaction to fire of cross-laminated timber in a controlled-atmosphere cone calorimeter, Fire Technol. 61 (1) (2025) 3–28.
[75] A. Battig, J.C. Markwart, F.R. Wurm, B. Schartel, Hyperbranched phosphorus flame retardants: multifunctional additives for epoxy resins, Polym. Chem. 10 (31) (2019) 4346–4358.
[76] A. Kumar, L.A. Connal, Biobased transesterification vitrimers, Macromol. Rapid Commun. 44 (7) (2023) 2200892.
[77] D. Reisinger, S. Kaiser, E. Rossegger, W. Alabiso, B. Rieger, S. Schlögl, Introduction of photolatent bases for locally controlling dynamic exchange reactions in thermo-activated vitrimers, Angew. Chem. Int. Ed. 60 (26) (2021) 14302–14306.
[78] R. Sayad, A. Bouzina, Y.O. Bouone, D. Beldjezzia, A. Djemel, M. Ibrahim-Ouali, et al., Zinc acetate-catalyzed, green and efficient synthesis of xanthene derivatives under ultrasound irradiation: X-ray crystallographic analysis and in silico study, RSC Adv. 14 (34) (2024) 24585–24603.
[79] A. Bifulco, S. Gaan, D. Price, A.R. Horrocks, Thermal decomposition of flame retardant polymers, in: Fire Retardancy of Polymeric Materials, CRC Press, 2024, pp. 11–35, https://doi.org/10.1201/9781003380689-2.
[80] D. Montarnal, M. Capelot, F. Tournilhac, L. Leibler, Silica-like malleable materials from permanent organic networks, Science 334 (6058) (2011) 965–968.
[81] M. Capelot, M.M. Unterlass, F. Tournilhac, L. Leibler, Catalytic control of the vitrimer glass transition, ACS Macro Lett. 1 (7) (2012) 789–792.
[82] J.P. Brutman, P.A. Delgado, M.A. Hillmyer, Polylactide vitrimers, ACS Macro Lett. 3 (7) (2014) 607–610.
[83] W. Denissen, G. Rivero, R. Nicolaÿ, L. Leibler, J.M. Winne, F.E. Du Prez, Vinylogous urethane vitrimers, Adv. Funct. Mater. 25 (16) (2015) 2451–2457.